Radiology
radiology.rsna.org

doi: 10.1148/radiol.10081634
February 2011 Radiology, 258, 351-369.

Principles of and Advances in Percutaneous Ablation

Muneeb Ahmed, MD, Christopher L. Brace, PhD, Fred T. Lee Jr, MD and S. Nahum Goldberg, MD

From the Laboratory for Minimally Invasive Tumor Therapy (M.A., S.N.G.), Section of Interventional Radiology (M.A.), and Section of Abdominal Imaging (S.N.G), Department of Radiology, Beth Israel Deaconess Medical Center, Harvard Medical School, 1 Deaconess Rd, Boston, MA 02215; Departments of Radiology and Electrical and Computer Engineering, University of Wisconsin Madison, Madison, Wis (C.L.B., F.T.L.); and Division of Image-guided Therapy, Department of Radiology, Hadassah Hebrew University Medical Center, Jerusalem, Israel (S.N.G.).
Address correspondence to
M.A. e-mail: (mahmed@bidmc.harvard.edu).

Abstract

Image-guided tumor ablation with both thermal and nonthermal sources has received substantial attention for the treatment of many focal malignancies. Increasing interest has been accompanied by continual advances in energy delivery, application technique, and therapeutic combinations with the intent to improve the efficacy and/or specificity of ablative therapies. This review outlines clinical percutaneous tumor ablation technology, detailing the science, devices, techniques, technical obstacles, current trends, and future goals in percutaneous tumor ablation. Methods such as chemical ablation, cryoablation, high-temperature ablation (radiofrequency, microwave, laser, and ultrasound), and irreversible electroporation will be discussed. Advances in technique will also be covered, including combination therapies, tissue property modulation, and the role of computer modeling for treatment optimization.

Learning Objectives

After reading the article and taking the test, the reader will be able to:

- Review the principles of focal tumor ablation, including the concept of complete treatment and achieving an ablative margin.

- Discuss the principles underlying the use of different types of ablative modalities.

• Describe the rationale and current status of tumor ablation combined with adjuvant therapies (eg, chemotherapy and radiation therapy).

Accreditation and Designation Statement

The RSNA is accredited by the Accreditation Council for Continuing Medical Education (ACCME) to provide continuing medical education for physicians. The RSNA designates this education activity for a maximum of 1.0 *AMA PRA Category 1 Credit™*. Physicians should only claim credit commensurate with the extent of their participation in the activity.

Disclosure Statement

The ACCME requires that the RSNA, as an accredited provider of CME, obtain signed disclosure statements from authors, editors, and reviewers for this case. For this educational activity, C.L.B. and F.T.L. disclosed relationships with Neuwave Medical; S.N.G. disclosed a relationship with AngioDynamics; M.A., the editor, and the reviewers indicated that they have no relevant relationships to disclose.

Introduction

Image-guided minimally invasive ablative therapies delivered by using needlelike applicators include both thermal (ie, radiofrequency [RF], microwave, laser, and cryoablation) and nonthermal (ie, chemical ablation and irreversible electroporation) techniques. These therapies have gained widespread attention and, in many cases, broad clinical acceptance as methods for treating focal malignancies in a wide range of tumor types and tissues, including primary and secondary malignancies of the liver, kidney, lung, and bone (1–6). Limitations in the success of focal therapies for treatment of certain tumor types and sizes have been reported, but researchers in several studies (7–10) have reported success by combining percutaneous therapies with other oncologic treatment strategies, including chemotherapy, radiation therapy, and transcatheter arterial therapy.

Given the rising complexity of treatment options and the expanding paradigms in interventional oncology, a thorough understanding of the basic principles of commonly used therapies is a prerequisite to being able to effectively provide treatment to these patients and to accurately interpret the many imaging studies that these patients undergo. Our article will highlight the various aspects and therapies of interventional oncology. We will provide a conceptual framework for the broad basic principles and underlying rationale that govern focal tumor therapies and percutaneous oncologic intervention. We will discuss the general principles of several commonly used thermal and nonthermal therapies in detail, including recent technologic advances. Current and future directions of research will also be reviewed, including modulation of tumor environment to enhance ablative therapies and the role of combining percutaneous therapies with other adjuvant therapies, such as chemo- and radiation therapy, with a focus on the

underlying mechanisms and principles guiding the potential synergy of combined treatments.

Expand

Goals of Minimally Invasive Tumor Ablation

Minimally invasive tumor ablation therapy for focal malignancies encompasses several specific objectives. Most importantly, through the application of energy or chemicals, the primary goal of most ablation procedures is to eradicate all viable malignant cells within a designated target volume. On the basis of examinations of tumor progression in patients undergoing surgical resection and the demonstration of viable malignant cells beyond visible tumor boundaries, in most cases (unless otherwise indicated), tumor ablation therapies are intended to include at least a 0.5–1.0-cm ablative margin of seemingly normal tissue for liver and lung, though less may be needed for some tumors in the kidney (11,12). While complete tumor eradication is of primary importance, sparing normal surrounding tissues and accuracy of therapy are always required. As such, one substantial advantage of percutaneous ablative therapies over conventional surgical resection is the potential to remove or destroy only a minimal amount of normal tissue. For example, in primary liver tumors, where functional hepatic reserve is a primary predictive factor for long-term patient survival outcome, ablation therapies can minimize iatrogenic damage to surrounding cirrhotic parenchyma (13). This is also useful when nephron-sparing treatments are needed in patients with von Hippel–Lindau syndrome, who are prone to the development of multiple renal cell carcinomas (14), and in patients with primary lung malignancies in the setting of extensive underlying emphysema and limited lung function (15,16). Other clinical circumstances in which high specificity and accuracy of targeting have proved useful include providing symptomatic relief for patients with symptomatic osseous metastases or hormonally active neuroendocrine tumors and using percutaneous therapies to improve focal interstitial drug delivery (10,17,18). Percutaneous thermal therapies are limited, however, by the quality of imaging guidance and, in some cases, by complex anatomy and difficult access.

Another important factor is that the amount of tumor destruction is determined by the pattern of distribution within treated tissues. This means that, for larger tumors (usually defined as greater than 3 cm in diameter), a single ablation treatment may not be sufficient to entirely encompass the target volume. In these cases, multiple overlapping ablations or simultaneous use of multiple applicators may be required to successfully treat the entire tumor and ablative margin, though accurate targeting and applicator placement can often be technically challenging (19).

Chemical Ablation

Intratumoral administration of chemically ablative substances, such as ethanol and acetic acid, has been studied for the longest clinical follow-up periods of the percutaneous ablation techniques, particularly as it relates to the treatment of hepatocellular carcinoma (20–23). Chemical ablation is an attractive option in many developing region of the world because it is inexpensive and simple. Several investigators (24,25) have also documented similar or greater efficacy with intratumoral instillation of acetic acid

compared with ethanol. However, success of chemical ablation therapies in more solid adenocarcinomas has been limited by reported difficulty in achieving uniform diffusion of percutaneously injected drugs over larger tumor volumes. As a result, focal thermal ablation has replaced chemical ablation in many cases. Chemical ablation is now more typically used as an adjuvant agent in tumors that are difficult to treat with thermal therapies, as a single agent in the treatment of smaller subcutaneous tumors (eg, locally recurrent thyroid cancer), or in treating focal benign lesions (eg, bronchogenic cysts, thyroglossal duct cysts, or endometriomas) (26–28).

Expand

Percutaneous ethanol instillation is principally used for treating hepatocellular carcinoma in patients with cirrhosis (29,30) (Fig 1). The injection of ethanol destroys tissue by two primary mechanisms: *(a)* as it diffuses into neoplastic cells, alcohol results in immediate dehydration of the cytoplasm, protein denaturation, and consequent coagulation necrosis and *(b)* alcohol entering the local circulation leads to necrosis of the vascular endothelium and subsequent platelet aggregation, resulting in vascular thrombosis and, ultimately, ischemic tissue necrosis (31,32). The treatment of primary hepatocellular carcinoma with ethanol injection has been considerably more successful than the treatment of liver metastases because of tumor characteristics, including softer tissue composition compared with the heterogeneous and dense fibrous nature of metastases and a capsule or pseudocapsule surrounded by cirrhotic liver, that limit diffusion and increase concentration within the target (33). Efficacy rates of ethanol instillation for hepatic metastases are poor, and it is therefore not recommended for the treatment of such malignancies. Given the several limitations of ethanol instillation, including poor and uneven distribution and limited success in a wider range of tumor types, researchers in several studies (24,25) have investigated the use of acetic acid as a viable injectable alternative to ethanol for cases requiring chemical ablation. The mechanisms of tissue injury are similar for both acetic acid and ethanol (34), though results of preliminary animal studies suggest that the diffusion abilities of acetic acid solutions may exceed those of ethanol, especially through fibrous tissues (35).

View larger version:

In this page In a new window

Download as PowerPoint Slide

Figure 1a:

(a) For ethanol ablation, a 21-gauge needle is used to inject ethanol into the tumor after placement with ultrasonographic or computed tomographic (CT) guidance. **(b)** Gross pathologic cross-section shows gross effects of ethanol instillation in a primary hepatic tumor. **(c)** Pretreatment contrast agent–enhanced axial CT image shows a focal hepatocellular carcinoma (arrow) in the right hepatic lobe, and **(d)** CT image obtained 3 months after ethanol instillation shows focal tumor necrosis with minimal peripheral enchancement (arrow).

Figure 1b:

Expand

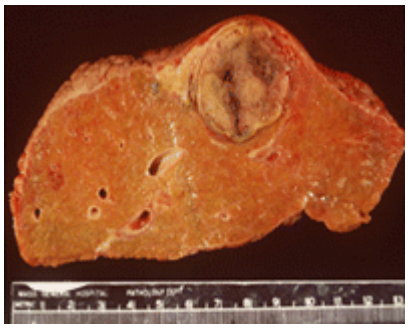

View larger version:
In this page In a new window
Download as PowerPoint Slide

(a) For ethanol ablation, a 21-gauge needle is used to inject ethanol into the tumor after placement with ultrasonographic or computed tomographic (CT) guidance. **(b)** Gross pathologic cross-section shows gross effects of ethanol instillation in a primary hepatic tumor. **(c)** Pretreatment contrast agent–enhanced axial CT image shows a focal hepatocellular carcinoma (arrow) in the right hepatic lobe, and **(d)** CT image obtained 3 months after ethanol instillation shows focal tumor necrosis with minimal peripheral enchancement (arrow).

View larger version:
In this page In a new window
Download as PowerPoint Slide

Figure 1c:

(a) For ethanol ablation, a 21-gauge needle is used to inject ethanol into the tumor after placement with ultrasonographic or computed tomographic (CT) guidance. **(b)** Gross pathologic cross-section shows gross effects of ethanol instillation in a primary hepatic tumor. **(c)** Pretreatment contrast agent–enhanced axial CT image shows a focal hepatocellular carcinoma (arrow) in the right hepatic lobe, and **(d)** CT image obtained 3 months after ethanol instillation shows focal tumor necrosis with minimal peripheral enchancement (arrow).

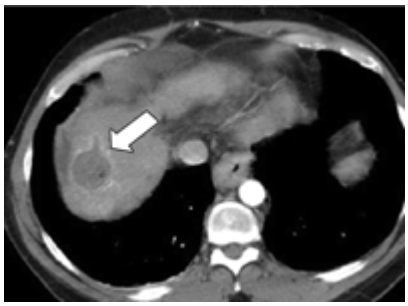

View larger version:
In this page In a new window
Download as PowerPoint Slide

Figure 1d:

(a) For ethanol ablation, a 21-gauge needle is used to inject ethanol into the tumor after placement with ultrasonographic or computed tomographic (CT) guidance. **(b)** Gross pathologic cross-section shows gross effects of ethanol instillation in a primary hepatic tumor. **(c)** Pretreatment contrast agent–enhanced axial CT image shows a focal hepatocellular

carcinoma (arrow) in the right hepatic lobe, and **(d)** CT image obtained 3 months after ethanol instillation shows focal tumor necrosis with minimal peripheral enchancement (arrow).

Expand

Thermal Ablation Therapies

Thermal ablation strategies attempt to destroy tumor tissue by increasing or decreasing temperatures sufficiently to induce irreversible cellular injury. These strategies can be broadly divided into cryoablation or hyperthermic ablation, in which heat may be generated by ultrasound or electromagnetic (ie, RF, microwave, laser) energy. Other techniques to generate heat or otherwise induce cellular necrosis have been reported; however, none have found widespread use to date (36–38). For the purposes of this review, we will consider only percutaneous energy-based ablation modalities, with emphasis given to those in widespread clinical use.

Complete and adequate destruction by thermal ablation requires that the entire tumor and an ablative margin be subjected to cytotoxic temperatures. The ability to heat or cool large volumes of tissue in different environments is dependent on several factors as follows: “the extent of coagulation necrosis induced in a given lesion is equal to the energy deposited, modified by local tissue interactions, minus the heat lost before inducing thermal damage” (39). On the basis of this relationship, several strategies have been developed to increase the amount of coagulation necrosis, including increasing energy deposition, modulating tissue characteristics, and modifying tissue blood flow. Again, although this is a useful framework, the absolute temperature achieved at any point within a tumor does not mean definitively that ablation has occurred, and heterogeneity of heating throughout the target volume is more often the rule than the exception.

Cryoablation

While early cryotherapy systems were bulky and limited to open surgical use, modern systems use more advanced cooling techniques that allow laparoscopic and percutaneous approaches in combination with imaging guidance. Common clinically treated tumors include focal primary renal tumors and palliative treatment of osseous metastases (17,40).

Recent advances in design and construction have allowed the use of smaller cryoprobes that are more appropriate for percutaneous procedures (diameter less than 13-gauge). However, it is important to note that the size of the ablation zone correlates to probe diameter in these systems; that is, cryoprobes with a smaller diameter typically create smaller zones of complete ablation. For example, 13-gauge (2.4-mm diameter) cryoprobes from one manufacturer (Endocare, Irvine, Calif) can be expected to produce zones of ablation approximately 2.5 cm in diameter in normal liver and lung tissues, while 15-gauge (1.7-mm diameter) probes will create 1.5–2.0-cm zones of ablation in these same organs (41–44). For this reason, many users choose to use two or more cryoprobes in proximity to ensure complete coverage of the tumor within the lethal isotherm. Thermal synergy between

cryoprobes has been shown to improve efficacy in both numeric and experimental tissue models, though inappropriate spacing in a given tissue type may lead to clefts between zones of ablation (43,45).

Expand

Current cryoablation systems use the Joule–Thomson effect to create unique freeze and thaw cycles. The Joule–Thomson effect describes the change in temperature of a gas resulting from expansion or compression of that gas. Argon is one example of a gas that cools during expansion; helium warms. Gas expansion occurs in a small chamber inside the distal end of the cryoprobe to create the necessary heat sink during freeze cycles and heat source during thaw cycles (Fig 2). Argon provides a heat sink of about 9 kJ and can generate temperatures as low as −140°C inside the iceball, which expands by thermal conduction (46). However, the fact that the lethal isotherm (−20° to −40°C) rests several millimeters inside of the iceball boundary must be considered when using imaging to assess cryoablation treatment efficacy (42).

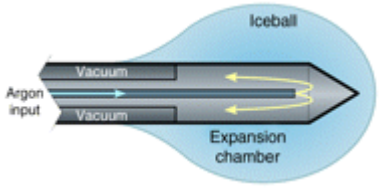

View larger version:
In this page In a new window
Download as PowerPoint Slide

Figure 2a:

(a) Schematic illustration of a cryoprobe tip with surrounding iceball formation. **(b)** Axial contrast-enhanced CT image shows iceball formation during cryoablation of a hepatic tumor in the right lobe by using multiple cryoprobes.

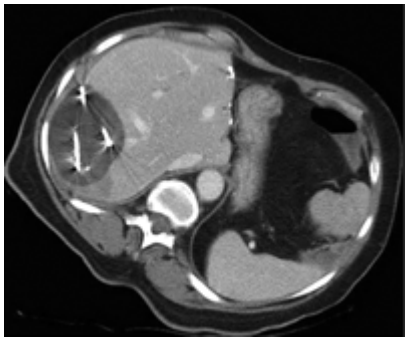

View larger version:
In this page In a new window
Download as PowerPoint Slide

Figure 2b:

(a) Schematic illustration of a cryoprobe tip with surrounding iceball formation. **(b)** Axial contrast-enhanced CT image shows iceball formation during cryoablation of a hepatic tumor in the right lobe by using multiple cryoprobes.

Another new system under development uses nitrogen near its critical point to provide lethal cooling, which may be more efficacious than Joule–Thomson–based systems (47). The critical point of a material describes a specific pressure and temperature where the distinction between gas and liquid phases vanishes. At this critical point, many materials (eg, nitrogen) can exhibit heat capacities that are orders of magnitude higher than water

while retaining the low viscosity of a gas. The result is a powerful cooling fluid that can be circulated through extremely small spaces, such as those inside a percutaneous cryoprobe. The increased cooling power of near-critical nitrogen may lead to smaller cryoprobes, eliminate the need for the large tanks now associated with argon- and helium-based cryoablation, and create larger zones of ablation than currently possible. However, substantial technical development and testing are needed to validate critical nitrogen cooling before clinical adoption is possible.

Expand

Hyperthermic Ablation

Thermal ablation of focal tumors uses high-temperature tissue heating (>50° C) surrounding applicators placed at the center of a tumor (Fig 3). Cellular homeostatic mechanisms can accommodate slight increases in temperature (up to 40°C). Although increased susceptibility to damage by other mechanisms (eg, radiation or chemotherapy, which will be discussed later) is seen at hyperthermic temperatures between 42° and 45°C, cell function and tumor growth continues even after prolonged exposure (48,49). Irreversible cellular injury occurs when cells are heated to 46°C for 60 minutes, and it occurs more rapidly as the temperature rises (50). Immediate cellular damage centers on protein coagulation of cytosolic and mitochondrial enzymes and nucleic acid-histone protein complexes (51–53). This damage triggers cellular death over the course of several days. The term *coagulation necrosis* is used to describe this thermal damage even though the manifestations of cell death following high-temperature thermal ablation may not fulfill strict histopathologic criteria of coagulative necrosis. For example, results of histopathologic studies (51,54) have demonstrated that tissues treated with RF ablation demonstrate immediate cessation of cytosolic and mitochondrial enzyme activity but may not demonstrate more classic findings of coagulative necrosis until at least several days later. This has implications with regard to clinical practice, as early posttreatment percutaneous biopsy and standard histopathologic interpretation may not be a reliable measure of adequate ablation. Optimal temperatures for ablation exceed 50°C and may be limited to 100°C for some applications (55). For example, tissue vaporization occurs at temperatures higher than 110°C, which, in turn, limits further current deposition in RF-based systems (compared with, for example, microwave systems, where higher temperatures do not interfere with deposition of energy).

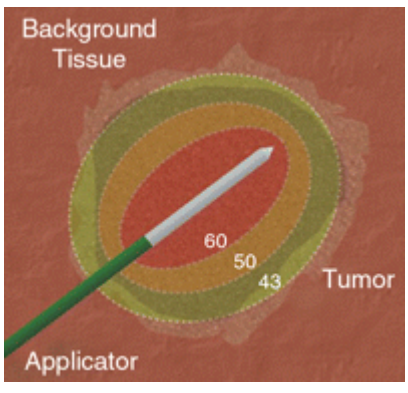

View larger version:
In this page In a new window
Download as PowerPoint Slide

Figure 3a:

(a) Schematic and **(b)** gross specimen show focal thermal ablation. Electrode applicators are positioned in the tumor with image guidance or direct visualization. A central zone of high temperatures (greater than 60°C, can exceed 100°C) is created in tissue immediately around the electrode, and it is

surrounded by more peripheral zones of sublethal tissue heating (43°–50°C) and background liver parenchyma.

Expand

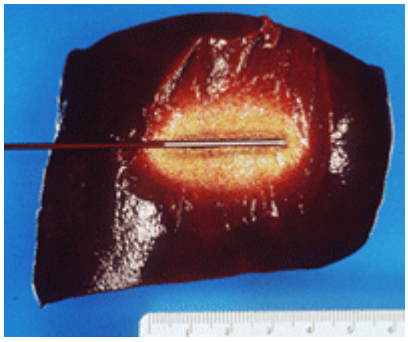

View larger version:

In this page In a new window

Download as PowerPoint Slide

Figure 3b:

(a) Schematic and **(b)** gross specimen show focal thermal ablation. Electrode applicators are positioned in the tumor with image guidance or direct visualization. A central zone of high temperatures (greater than 60°C, can exceed 100°C) is created in tissue immediately around the electrode, and it is surrounded by more peripheral zones of sublethal tissue heating (43°–50°C) and background liver parenchyma.

Despite the theoretical temperature construct presented in the preceding paragraph, the threshold target temperature of 50°C should be used only as a general guideline. Indeed, the exact temperature at which cell death occurs is multifactorial and tissue specific. On the basis of results of a study (55) that demonstrate that tissue coagulation can be induced by focal tissue heating to approximately 50°C for less than 5 minutes, this has become the standard surrogate endpoint for thermal ablation therapies in both experimental studies and current clinical paradigms. Researchers (56,57) have shown that, depending on heating time and the tissue being heated, maximum temperatures at the edge of ablation range in value. Maximum temperatures at the edge of the ablation zone, known as the critical temperature, have been shown to range from 30° to 77°C for normal tissues and from 41° to 64°C for tumor models (a 23°C difference) (Fig 4). Likewise, the thermal dose (ie, the total amount of heat administered for a given time) required to induce cell death varies significantly between different tissues (56).

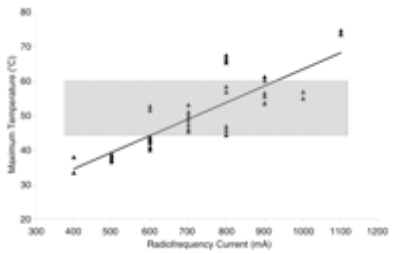

View larger version:

In this page In a new window

Download as PowerPoint Slide

Figure 4:

Graph of maximum temperature at ablation zone margin shows wider than expected variation, ranging from 33° to 76°C (56). Temperatures were monitored at 10–25 mm from the 2-cm internally cooled electrode during RF ablation (500 kHz generator; current, 400–

1100 mA varied in 100-mA intervals) of a fixed coagulation diameter in ex vivo bovine liver. Gray band = previously reported maximum range.

Expand

RF Ablation

By far, the most well-studied and clinically relevant percutaneous ablation source to date has been RF energy. As such, RF-based systems serve as a useful model for discussing thermal ablation in general and more specific advances in development (such as combination therapies, which are discussed later), findings of which can often be applied more broadly to other thermal technologies.

During RF ablation, electrical current from the generator oscillates between electrodes through ion channels present in most biologic tissues. In this way, the RF ablation setup can be thought of as a simple electrical circuit wherein the current loop comprises a generator, cabling, electrodes, and tissue as the resistive element. Tissues are imperfect conductors of electricity (they have electrical impedance), so current flow leads to frictional agitation at the ionic level and heat generation, known as the Joule effect. Heating occurs most rapidly in areas of high current density: Tissues nearest to an electrode are heated most effectively, while more peripheral areas receive heat by thermal conduction (58).

As noted in earlier sections, ablative heating leads to tissue dehydration and water vaporization, which cause dramatic increases in circuit impedance (59). These rapid and often sudden increases in impedance can be used as a feedback signal in RF generators, which will be covered in more detail later. When these effects begin to inhibit current flow from a generator, alternative methods to decrease circuit impedance, such as expanding the electrode surface area, pulsing the input power, and injections of saline, can be used to augment RF current flow (60,61).

Electrodes.—While any conductor and power source can create a thermal ablation, the power output and control algorithms for each generator have been tailored to suit its associated electrodes. Most RF ablation systems today operate in a monopolar mode by using two different types of electrodes: interstitial electrodes (hereafter, electrode) and dispersive electrodes on the skin surface (also known as ground pads). The electrode delivers energy to the tumor, creating a volume of high current density and localized heating. The ground pad closes the electrical current path but is designed to disperse energy over a large surface area to reduce the likelihood of thermal injury to the skin.

Monopolar electrode designs include both straight insulated needles with an exposed metallic tip and multitined electrodes. Internally cooled electrodes use a single needle, in which fluid is circulated inside the electrode's active tip, and temperatures at the electrode-tissue interface are reduced. Lower temperatures inhibit charring, which, in turn, allows increased power deposition. In effect, internal cooling drives RF heating from the electrode-tissue interface deeper into the tissue to create more clinically relevant

ablations (approximately 2 cm in diameter in normal liver) (62,63). When using water as a cooling fluid, the initial temperature of the water does not seem to affect device performance (64). The cooled needle design also uses a smaller caliber applicator (17 gauge, 1.5-mm diameter) compared with expandable electrodes. Internally cooled needles are now used by the Cool-tip system (Valleylab by Covidien, Boulder, Colo).

Expand

In contrast, electrodes with multiple tines emanating from a single electrode sheath or handle assembly aim to distribute energy spatially (65,66) (Fig 5). The use of multiple tines improves heating efficiency in the target volume and also increases total electrode surface area, thereby reducing circuit impedance and promoting greater energy deposition. As a result, larger zones of ablation and potentially faster heating can be achieved (67). One type of multitined electrode utilizes three single 17-gauge electrodes, which are spaced 5 mm apart in a triangular configuration and driven in parallel by the same generator source. This configuration effectively behaves as a single larger electrode, but it has a limited puncture area and can create zones of ablation over 3 cm in diameter in normal liver in 12 minutes with a 200-W generator (65). The Cluster electrode system is an example of a nondeployable multitined electrode.

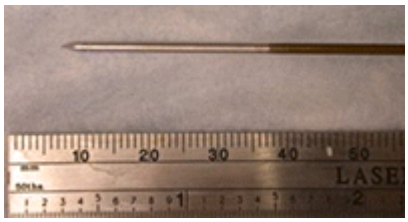

View larger version:
In this page In a new window
Download as PowerPoint Slide

Figure 5a:
Images of various commonly used and commercially available RF electrode designs. **(a)** Single internally cooled electrode with a 3-cm active tip (Cool-tip system). **(b)** Cluster internally cooled electrode system with three 2.5-cm active tips (Cluster electrode system; Valleylab). Two variations of an expandable electrode system: **(c)** StarBurst (RITA/AngioDynamics, Fremont, Calif) and **(d)** LeVeen (Boston Scientific, Natick, Mass).

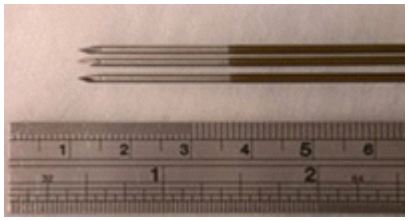

View larger version:
In this page In a new window
Download as PowerPoint Slide

Figure 5b:
Images of various commonly used and commercially available RF electrode designs. **(a)** Single internally cooled electrode with a 3-cm active tip (Cool-tip system). **(b)** Cluster internally cooled electrode system with three 2.5-cm active tips (Cluster electrode system; Valleylab). Two variations of an expandable electrode system: **(c)** StarBurst

(RITA/AngioDynamics, Fremont, Calif) and **(d)** LeVeen (Boston Scientific, Natick, Mass).

Expand

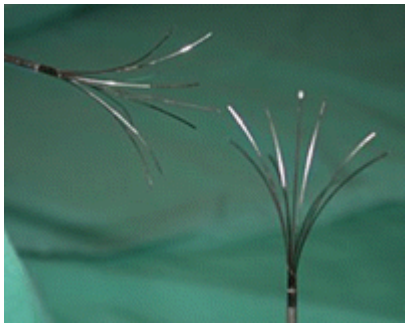

View larger version:
In this page In a new window
Download as PowerPoint Slide

Figure 5c:
Images of various commonly used and commercially available RF electrode designs. **(a)** Single internally cooled electrode with a 3-cm active tip (Cool-tip system). **(b)** Cluster internally cooled electrode system with three 2.5-cm active tips (Cluster electrode system; Valleylab). Two variations of an expandable electrode system: **(c)** StarBurst (RITA/AngioDynamics, Fremont, Calif) and **(d)** LeVeen (Boston Scientific, Natick, Mass).

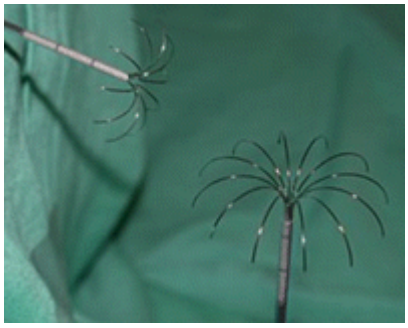

View larger version:
In this page In a new window
Download as PowerPoint Slide

Figure 5d:
Images of various commonly used and commercially available RF electrode designs. **(a)** Single internally cooled electrode with a 3-cm active tip (Cool-tip system). **(b)** Cluster internally cooled electrode system with three 2.5-cm active tips (Cluster electrode system; Valleylab). Two variations of an expandable electrode system: **(c)** StarBurst (RITA/AngioDynamics, Fremont, Calif) and **(d)** LeVeen (Boston Scientific, Natick, Mass).

Other multitined electrode designs deploy several smaller electrodes from a single needle shaft (66). Two such designs are clinically available today that create either star- or umbrella-shaped arrays. Star-shaped electrodes are deployable from a 14-gauge (2.1-mm diameter) needle in arrays of four, nine, or 12 tines. Many such electrodes also use hollow tines capable of being used to inject saline into the surrounding tissue to reduce impedance and increase energy delivery. Umbrella-shaped electrodes, on the other hand, contain 10 tines and are deployed from a 13-gauge needle. These tines are electrically connected and operate in parallel, which means that current flowing through each tine can vary depending upon local tissue properties. Deployable electrodes are capable of creating zones of ablation

approximately 3–4 cm in diameter, though care should be taken when evaluating device performance since deployable designs have also been associated with irregular heating patterns (68). In general, multitined electrodes are more invasive and may increase complication rates, especially in percutaneous settings, though relevant comparisons between devices are lacking (69,70). Introduction or retraction complications with deployable electrodes have been reported but are relatively rare (71). Examples of multitined deployable designs include the Starburst and LeVeen electrodes.

Alternatively, in bipolar systems, current oscillates between two interstitial electrodes without the need for a ground pad (72,73). The electrodes may lie on separate applicators or be situated longitudinally along the same applicator. The bipolar setup restricts current flow primarily to the area between the electrodes and protects this area from perfusion-mediated cooling, resulting in faster more focal heating between the electrodes. Bipolar operation may require more precise placement of the electrodes to create a confluent zone of necrosis and can be limited by local changes in conductivity resulting from the ablation (72). For this reason, bipolar systems often use saline infusion to increase energy delivery between the electrodes. Multipolar operation has also become available, which involves switching between pairs of bipolar electrodes situated on individual needles (74,75). The ProSurge system (Celon; Teltow, Germany) is an example of a multipolar device.

Generator and ground pads.—The RF ablation generator provides three essential functions: power generation, control, and user interface. It is important to remember that an RF ablation system can be approximated as a basic resistor circuit and that current is governed by Ohm's law: $I = V/Z$, where I is current in amperes, V is voltage in volts, and Z is impedance (Ω) in ohms. Power, P, is defined as the product of voltage and current: $P = VI = V^2/Z = I^2Z$. Power output is controlled by the output voltage and circuit impedance, which includes all possible factors, such as electrode design, target tissue environment, background tissue properties, and ground pad connectivity. Since power depends on impedance, RF ablation may be limited in areas of high background impedance, such as the lung, even if the tumor exhibits a relatively high conductivity (76,77). As tissue impedance rises, power output tends to decrease. Generators are now available from 150 to 250 W, which may be underpowered for some clinical scenarios (eg, in lung). Higher-power designs are currently under development to address these problems (78,79).

The most important distinguishing factor between commercially available generators is in the feedback and control system. Both impedance-based and electrode temperature-based controls are available. In the Boston Scientific system, power is set initially at a relatively low level (typically 20–50 W) and gradually increased until impedance elevates to near-infinite levels. In the Valleylab system, initial power is usually set to the maximum level. When the circuit impedance spikes rapidly, the generator turns off RF power for a short period to facilitate tissue cooling and rehydration, which allows more power to be used when the generator switches back on. This power pulsing algorithm has been shown to increase ablation zone size and decrease treatment time (80,81).

Switching between multiple electrodes on the basis of impedance spikes uses the inherent off time of the power pulsing algorithm to deliver energy through another electrically independent electrode (82). Up to three equivalent ablations can be created independently in the same time as a single-electrode ablation, or a closely spaced array can be used to create large conglomerate ablations with substantial time savings over the technique of overlapping single-electrode ablations (83,84).

Electrode tip temperatures are also monitored in some systems; however, only the RITA/AngioDynamics system uses that information to control power output. In that system, generator output is ramped up until electrode temperatures reach a predetermined value, usually around 95°C, and maintained at this temperature for typically 20–30 minutes. This power delivery strategy works effectively with multiple-tine electrode designs because of the dispersion in current density and large electrode surface area.

The ground pad used with monopolar electrodes is intended to provide a large dissipative surface for electrical current flow through the skin. However, most of the current tends to congregate around the edge of the pad nearest to the interstitial electrode, and skin burns can result from uneven placement or insufficient number of pads (2,85,86). In practice, given the substantial attention to this problem, ground pad burns are rarely a problem. Nevertheless, as more RF energy is being applied per procedure with higher power and multiple-electrode systems, ground pad loads are also increasing. Strategies to prevent ground pad burns include monitoring temperature and impedance through each pad, cooling the pad, optimized pad designs, and switching between pads to reduce heating (87).

Microwave Ablation

The term *microwave* describes electromagnetic energy in the 300 MHz to 300 GHz range; however, for practical and regulatory reasons, microwave ablation devices are typically operated at either 915 MHz or 2.45 GHz. Microwave heating is produced as a result of dielectric hysteresis (rotating dipoles), which differs from the Joule heating mechanism of RF ablation. When electromagnetic energy is applied to tissue, some of the energy is used to force molecules with an intrinsic dipole moment (eg, water) to continuously realign with the applied field. This rotation of molecules represents an increase in kinetic energy and, hence, an elevation in local tissue temperatures. As such, microwave energy has demonstrated several advantages for tissue ablation (88,89). Microwaves readily penetrate through biologic materials, including those with low electrical conductivity, such as lung, bone, and dehydrated or charred tissue. Consequently, microwave power can be continually applied to produce extremely high (>150°C) temperatures, which improves ablation efficacy by increasing thermal conduction into the surrounding tissue (90). Microwaves also heat tissue more efficiently than does RF energy, microwaves do not require ground pads, and multiple antennas can be operated simultaneously (91). The superposition of microwaves may even be exploited to augment performance (92–95).

On the other hand, microwave energy is inherently more difficult to distribute than RF energy. Microwaves must be carried in waveguides, such

as coaxial cable, which are typically more cumbersome than the small wires used to feed energy to RF electrodes and are prone to heating when carrying large amounts of power. It is well known that higher microwave powers increase ablation zone size, but excessive power in the antenna shaft can lead to unintended injuries to other tissues, such as the skin (88,96). Recent investigations have shown that adding a cooling jacket around the antenna can reduce cable heating and eliminate skin burns while effectively increasing the amount of power that can safely be delivered to the tumor (97).

Expand

The purpose of the antenna is to couple energy from the feeding cable into the tissue. Antenna designs vary, and trade-offs between antenna efficiency, size, and heating pattern are often required (98) (Fig 6). Antenna properties, such as efficiency and heating pattern, are primarily controlled by the surrounding tissue properties and antenna geometry. Common designs include monopole, dipole, triaxial, choked, and slotted antennas. Most antennas use a straight needlelike design, though deployable loops have also been reported (99).

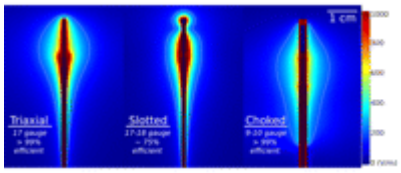

View larger version:

In this page In a new window

Download as PowerPoint Slide

Figure 6:

Images show electric field patterns surrounding three microwave antenna designs with associated antenna size and power-application efficiency: triaxial, single slot *(Slotted)*, and choked dipole *(Choked)*. Energy distribution, in volts per meter, is color coded for simulations at 2.45 GHz and 50-W input power in normal liver tissue. Images show the balance between antenna size, efficiency, and heating pattern. For example, heating can be localized to the distal antenna tip by adding a choke coil at the expense of increased invasiveness (9–10 gauge, which is not suitable for percutaneous application). Thinner antennas can also be created but typically sacrifice efficiency (see slotted design). (Reprinted, with permission, from reference 141.)

Microwave ablation has been used the most in Japan and China, where several systems have been described (100,101). Most of these systems operate at 2.45 GHz and use monopole, dipole, or slotted coaxial antennas to deliver up to 60 W. Recently, 915-MHz and water-cooled systems have been described, which appear to deliver up to 80 W and create larger ablation zones than do previous systems (102). Currently, only one system (Evident; Valleylab) has been approved by the Food and Drug Administration and is being actively marketed for percutaneous microwave tumor ablation in the United States. It comprises a water-cooled 13-gauge dipole antenna coupled to a 915-MHz generator with a maximum output power of 45 W. Other systems are currently in development worldwide and will likely see clinical launch in the next few years.

Laser Ablation

Laser ablation is familiar to many for treating skin disorders or corrective procedures in the eye, but similar generator technologies and specially designed applicators have allowed lasers to be used for interstitial tumor ablation as well (103,104) (Fig 7). Laser sources, including pumped neodymium-doped yttrium aluminum garnet and semiconductor diodes that emit approximately 600–1000-nm wavelength light energy, can be found in most clinical centers, but they are rarely used for thermal tumor ablation. Adoption outside of a few centers in Europe has been relatively weak compared with RF and cryoablation, in part owing to a lack of Food and Drug Administration–approved systems, sparse availability of applicators, and few performance advantages over existing RF, microwave, and cryoablation systems (105).

View larger version:
In this page In a new window
Download as PowerPoint Slide

Figure 7a:
Images of **(a)** laser ablation diffuser tip and **(b)** shaft with cooling. Laser energy is passed through an optical fiber, which may be cooled along its length to prevent heating proximal to the target zone. Diffuser tip (pink line in **a**) scatters light into a larger volume of tissue than an end-fire catheter to create larger and more uniform zones of ablation. (Images courtesy of Thomas Vogl, MD, University Hospital Frankfurt, Johann Wolfgang Goethe University, Frankfurt, Germany.)

View larger version:
In this page In a new window
Download as PowerPoint Slide

Figure 7b:
Images of **(a)** laser ablation diffuser tip and **(b)** shaft with cooling. Laser energy is passed through an optical fiber, which may be cooled along its length to prevent heating proximal to the target zone. Diffuser tip (pink line in **a**) scatters light into a larger volume of tissue than an end-fire catheter to create larger and more uniform zones of ablation. (Images courtesy of Thomas Vogl, MD, University Hospital Frankfurt, Johann Wolfgang Goethe University, Frankfurt, Germany.)

Like RF and microwave energy, lasers induce electromagnetic heating to elevate tissue temperatures to lethal levels. The primary advantage of using laser energy is that it may be coupled through optical fibers, which are inherently magnetic resonance (MR) imaging compatible. In addition, the lack of metal in the power distribution chain and relatively small diameter of most

applicators effectively eliminate image artifacts on CT and MR images. Thus, it is more reasonable to perform MR temperature mapping during laser ablation (106).

Laser light is an efficient and precise energy source for tissue heating. However, because light is scattered and absorbed rapidly by most body tissues, lasers have limited energy penetration and create smaller ablation zones (1–2-cm diameter) than many other devices currently in use (107). Light does not penetrate through charred or desiccated tissues. Diffuser tips are used to improve applicator heating profiles, and higher powers can offset the reduced penetration depth by increasing local temperatures, but when higher powers are used, fibers must be cooled to avoid skin burns or probe failure (108). Cooling increases the diameter of each applicator. Larger ablation volumes are typically realized by using multiple applicators, which can be operated independently and simultaneously (109).

Emerging Technologies

Ultrasonic Ablation

In addition to the well-known transcutaneous uses of ultrasound, it is also possible to elevate tissue temperatures by using interstitial ultrasound applicators (110,111). Heating created by such applicators can be both directional and adjustable with proper amplitude and phase control of the transducer array elements (110,111). Highly directional power delivery gives interstitial ultrasound a distinctive ability to concentrate maximal heating in one sector to increase local heating with relatively high precision, and larger ablations may be realized by sweeping the active heating region through the target volume. The directivity of the applicator may also be used to protect critical structures while heating nearby tissues.

To date, the diameters of many of these devices have been larger than 13 gauge, falling outside the boundaries of what is normally considered acceptable for percutaneous tumor ablation; however, percutaneous devices have been investigated (110,111). Recent reports in animal prostate models have demonstrated the potential of percutaneous interstitial ultrasound heating for interventional oncology, but almost no clinical experience exists (112).

Irreversible Electroporation

Percutaneous irreversible electroporation (IRE) is a relative newcomer to the field of tumor ablation and is most notable because it is inherently nonthermal; no heat is produced to cause cell death. Rather, cells are eradicated by using several microsecond-to-millisecond-long pulses of electrical current. The pulses generate electric fields up to 3 kV/cm, which cause irreversible damage to the cell membrane, thereby inducing apoptosis (113,114) (Fig 8). Since IRE is nonthermal, heat sinks, such as large vessels, should have a much smaller influence on the ablation zone than in thermal treatments. IRE also appears to limit damage to more collagenous tissues and nerves, which if verified in larger trials, will make it an attractive option

for thermally sensitive areas (eg, prostate, near large blood vessels, or renal cortex) (115).

Expand

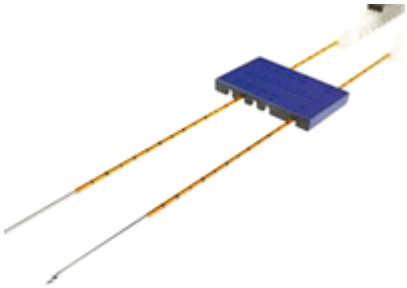

View larger version:

In this page In a new window

Download as PowerPoint Slide

Figure 8a:

(a) Monopolar IRE applicator and **(b)** bipolar IRE applicator with gross specimen of IRE ablation zone. Monopolar applicators create an electric field between pairs of electrodes, requiring multiple electrodes to be inserted. Bipolar applicators create an electric field between the two coaxial electrode sections. Gross specimen shows that there is no heat-sink effect in the IRE ablation zone, as coagulation extends up to and around the vessel lumen (arrows). (Images courtesy of William Hamilton, AngioDynamics.)

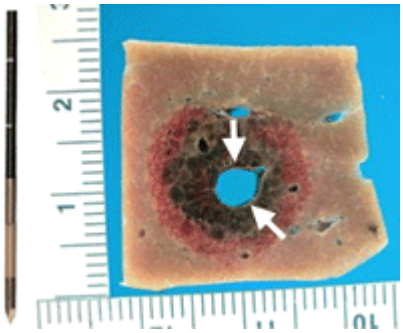

View larger version:

In this page In a new window

Download as PowerPoint Slide

Figure 8b:

(a) Monopolar IRE applicator and **(b)** bipolar IRE applicator with gross specimen of IRE ablation zone. Monopolar applicators create an electric field between pairs of electrodes, requiring multiple electrodes to be inserted. Bipolar applicators create an electric field between the two coaxial electrode sections. Gross specimen shows that there is no heat-sink effect in the IRE ablation zone, as coagulation extends up to and around the vessel lumen (arrows). (Images courtesy of William Hamilton, AngioDynamics.)

IRE electrodes consist of insulated 19-gauge (1.1-mm-diameter) or larger needles with an exposed active portion of 1-4 cm. For most applications, multiple electrodes are required, which are spaced 1-3 cm apart to provide sufficient electric field strengths for irreversible cell damage. A single-needle bipolar electrode is also available for more localized treatments. While initial studies required extremely high voltage pulses, a more recent report (116) has shown that lower voltage pulses can be used when repeated several hundred times.

Current IRE devices do have notable drawbacks, including generation of potentially dangerous electrical harmonics that can stimulate muscle contraction or cardiac arrhythmias. These techniques require general anesthesia and paralytic induction and have treatment times on the order of seconds, which prevent treatment monitoring or adjustment. There is also a requirement for accurate placement of several needles to achieve moderate-sized ablations (approximately 3–4 cm) and a lack of coagulation around the needle insertion sites, which theoretically could elevate bleeding complication risks. Ongoing research aims to minimize these complications.

Comparison of Technologies

While each thermal ablation energy source is unique, the goal of each is to elevate tissue temperatures enough to create zones of irreversible cellular damage. RF energy is relatively inexpensive and easy to generate, but it is limited by the need for electrical current flow. For this reason, RF ablation suffers in areas of high blood flow or high tissue impedance (eg, lung) and requires electrical switching for effective multiple-applicator use. Microwave heating is fast and efficient and, thus, appears better equipped to overcome heat sinks and treat large tumor volumes. Microwaves are also relatively tissue insensitive and offer improved multiple-applicator support, but they can be more difficult to distribute than other energy sources. Laser energy is also fast and relatively tissue insensitive, and generators are already available worldwide, but ablation applicators are not as common and perform about the same as established RF electrodes of similar size. Interstitial ultrasound devices offer better control of the applicator heating pattern but are typically too large for percutaneous use and are, so far, clinically unproved. Finally, operator technique may have as much influence on performance as device technology. For example, multiple applicators can be used to increase heating rather than switching to a different energy source. While some energy sources may be better suited to certain applications, none has proved itself a clear favorite for all applications.

Current and Future Research

Ablation research has historically focused on creating larger or more uniform zones of ablation that are reproducible in many situations through device and application development, but device engineering is always constrained by the physiology of the target. This section will describe new approaches to augment device performance by altering the underlying tissue physiology, optimizing energy delivery, or combining ablative therapies with other treatments, such as radiation or drug therapies, to increase ablation size, uniformity, or treatment specificity.

Modulating Tissue Characteristics

Many recent investigations have centered on altering underlying tumor physiology as a means to advance thermal ablation. Most studies to date have focused on the effects of tissue characteristics in the setting of temperature-based therapies in general, such as tissue perfusion and

thermal conductivity, and system-specific characteristics, such as electrical conductivity for RF-based ablation.

Expand

Tissue perfusion.—The foremost factor limiting thermal ablation of tumors continues to be tissue blood flow, which acts as a heat sink and reduces the volume of tissue heated to target temperature, either through large blood vessels or capillary-mediated perfusion. Larger diameter blood vessels (especially those greater than 3 mm in diameter) act as heat sinks, drawing away either heat or cold from the ablative area (Fig 9), and have higher patency rates, less endothelial injury, and greater viability of surrounding hepatocytes after RF ablation (117). The strong effects of hepatic blood flow have been confirmed in multiple studies where the zone of coagulation is increased when hepatic blood flow is reduced by using arterial embolization techniques (eg, balloons, coils, particles, or lipiodol agents). Researchers have also administered intraarterial and systemic pharmacologic agents, such as halothane and arsenic trioxide, to reduce tissue perfusion and, therefore, blood flow-mediated tissue cooling. Promising antiangiogenic therapies, such as sorafenib, are also starting to be studied as combination therapies with ablation, with similar encouraging results in animals (118) (Fig 10).

View larger version:

In this page In a new window

Download as PowerPoint Slide

Figure 9a:

Images show effect of blood flow on RF ablation size. **(a)** Gross bovine liver specimen shows how the heat-sink effect from a large hepatic vein (arrow) results in an incomplete zone of coagulation after in vivo RF ablation (3-cm single internally cooled electrode, 12-minute RF application). **(b)** Contrast-enhanced axial CT image shows how mechanical occlusion (ie, intraoperative portal vein occlusion with the Pringle maneuver) can increase RF coagulation size (upper ablation zone) by reducing the cooling effects of tissue perfusion as compared with the adjacent smaller ablation zone (arrow) that was obtained without the Pringle maneuver. (Part **b** reprinted, with permission, from reference 92.)

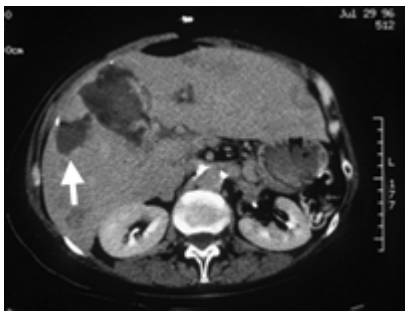

View larger version:

Figure 9b:

Images show effect of blood flow on RF ablation size. **(a)** Gross bovine liver specimen shows how the heat-sink effect from a large hepatic vein (arrow) results in an incomplete zone of coagulation after in vivo RF ablation (3-cm

In this page In a new window
Download as PowerPoint Slide

single internally cooled electrode, 12-minute RF application). **(b)** Contrast-enhanced axial CT image shows how mechanical occlusion (ie, intraoperative portal vein occlusion with the Pringle maneuver) can increase RF coagulation size (upper ablation zone) by reducing the cooling effects of tissue perfusion as compared with the adjacent smaller ablation zone (arrow) that was obtained without the Pringle maneuver. (Part **b** reprinted, with permission, from reference 92.)

View larger version:
In this page In a new window
Download as PowerPoint Slide

Figure 10a:

Gross specimens show increases in RF-induced coagulation (arrows) when combined with pharmacologic modulation of tissue and tumor blood flow versus RF ablation alone. **(a)** Rabbit kidneys show increased coagulation (arrows) when arsenic trioxide, which has known antivascular effects, is combined with RF ablation (right) versus RF ablation alone (left). (Reprinted, with permission, from reference 93.) **(b)** Mouse tumor model shows increased tumor coagulation zones (9 mm vs 4 mm; arrows) when sorafenib, a vascular endothelial growth factor receptor inhibitor, is combined with RF ablation (right) versus RF ablation alone (left). (Reprinted, with permission, from reference 118.)

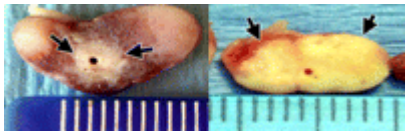

View larger version:
In this page In a new window
Download as PowerPoint Slide

Figure 10b:

Gross specimens show increases in RF-induced coagulation (arrows) when combined with pharmacologic modulation of tissue and tumor blood flow versus RF ablation alone. **(a)** Rabbit kidneys show increased coagulation (arrows) when arsenic trioxide, which has known antivascular effects, is combined with RF ablation (right) versus RF ablation alone (left). (Reprinted, with permission, from reference 93.) **(b)** Mouse tumor model shows increased tumor coagulation zones (9 mm vs 4 mm; arrows) when sorafenib, a vascular endothelial growth factor receptor inhibitor, is combined with RF ablation (right) versus RF ablation alone (left). (Reprinted, with permission, from reference 118.)

Thermal conductivity.—It was initially found that the use of RF ablation for hepatocellular carcinoma in underlying cirrhotic liver resulted in an oven effect (ie, increased heating efficacy for tumors surrounded by cirrhotic liver or fat) or altered thermal transmission at the junction of tumor tissue and surrounding tissue (119). Results of a subsequent experimental study (120) have confirmed the effects of varying tumor and surrounding tissue thermal conductivity on effective heat transmission during RF ablation. For example, poor tumor thermal conductivity limits heat transmission centrifugally away from the electrode, with marked heating in the central tumor and limited, potentially incomplete, heating in peripheral portions of the tumor. In contrast, increased thermal conductivity, such as that in cystic lesions, results in fast heat transmission (ie, heat dissipation), with potentially incomplete and heterogeneous tumor heating. Different tumor and organ characteristics may also make a 1-cm ablative margin difficult to achieve (120). Thus, an understanding of tissue and tumor thermal conductivities may be useful when trying to predict ablation outcome in varying clinical settings (eg, exophytic renal cell carcinomas surrounded by perirenal fat, lung tumors surrounded by aerated normal parenchyma, or osseous metastases surrounded by cortical bone) (120).

Electrical conductivity.—RF-induced tissue heating, generated by resistive heating from ionic agitation, is strongly dependent on the local electrical conductivity. Altering the electrical environment immediately around the RF electrode with ionic agents can increase electrical conductivity prior to or during RF ablation, allow greater energy deposition, and, therefore, increase coagulation volume (121,122) (Fig 11). Saline may also be of benefit when attempting to ablate cavitary lesions that might not otherwise contain a sufficient current path. In general, small volumes of highly concentrated sodium ions are injected in and around the ablation site to maximize local heating effects, which has been observed in both experimental and clinical studies and has been subsequently incorporated into electrode development (123). However, it should be noted that saline infusion is not always a predictable process since the fluid can migrate to unintended locations and cause complications if not used properly (124).

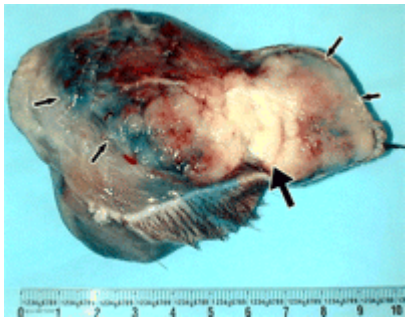

View larger version:
In this page In a new window
Download as PowerPoint Slide

Figure 11a:

Gross specimens show modulation of intratumoral electrical conductivity with adjuvant NaCl injection around the RF electrode increases RF-induced (1-cm single internally cooled electrode, 12-minute RF ablation) tissue coagulation in a subcutaneously implanted canine venereal sarcoma tumor model. **(a)** Tumor treated with RF ablation alone shows a 3.2-cm central focus of coagulation (large arrow) surrounded by marked hyperemia. Evans Blue, a marker for vascular perfusion, intensely stains the peripheral subcutaneous

tissues and residual unablated tumor (small arrows). **(b)** A 5.5-cm tumor treated with RF ablation and 36% NaCl solution pretreatment shows no evidence of residual vascular perfusion. Intense hyperemia and perfusion is seen in the cutaneous and peripheral tissues (arrows). However, no evidence of mitochondrial enzyme activity or perfusion was seen in this completely ablated tumor. (Reprinted, with permission, from reference 94.)

Expand

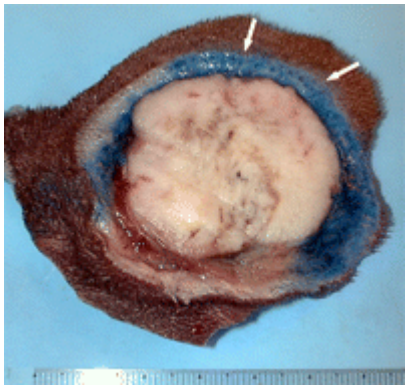

View larger version:

In this page In a new window

Download as PowerPoint Slide

Figure 11b:

Gross specimens show modulation of intratumoral electrical conductivity with adjuvant NaCl injection around the RF electrode increases RF-induced (1-cm single internally cooled electrode, 12-minute RF ablation) tissue coagulation in a subcutaneously implanted canine venereal sarcoma tumor model. **(a)** Tumor treated with RF ablation alone shows a 3.2-cm central focus of coagulation (large arrow) surrounded by marked hyperemia. Evans Blue, a marker for vascular perfusion, intensely stains the peripheral subcutaneous tissues and residual unablated tumor (small arrows). **(b)** A 5.5-cm tumor treated with RF ablation and 36% NaCl solution pretreatment shows no evidence of residual vascular perfusion. Intense hyperemia and perfusion is seen in the cutaneous and peripheral tissues (arrows). However, no evidence of mitochondrial enzyme activity or perfusion was seen in this completely ablated tumor. (Reprinted, with permission, from reference 94.)

Differences in electrical conductivity between the tumor and surrounding background organ can affect tissue heating at the tumor margin. Several studies have demonstrated increases in tissue heating at the tumor-organ interface when the surrounding medium is characterized by lower electrical conductivity (77). In certain clinical settings, such as when treating focal tumors in either lung or bone, marked differences in electrical conductivity may result in variable heating at the tumor-organ interface, may limit heating in the surrounding organ, and may make obtaining even a 1-cm ablative margin difficult.

Finally, nonionic fluids can be used to protect tissues adjacent to the ablation zone (eg, diaphragm or bowel) from thermal injury by using the technique commonly referred to as hydrodissection (125). For this application, fluids with low ion content, such as 5% dextrose in water, should be used because they have been proved to electrically force RF current away from the

protected organ, decrease the size and incidence of burns on the diaphragm and bowel, and reduce pain scores in patients treated with 5% dextrose in water when compared with ionic solutions, such as saline (126). Ionic solutions (eg, 0.9% saline) should not be used for hydrodissection because, as noted above, they actually increase RF current flow (126).

Effect of Tissue Composition on Other Energy Sources

In addition to the characteristics generally applicable to heat-based therapies (eg, thermal conductivity) and similar to the effect of electrical conductivity on RF ablation, tissue characteristics are likely to influence outcomes in other energy-based ablation technologies. For example, dielectric properties like relative permittivity (how well a material will store charge) and bulk conductivity (the energy loss inside the material) influence microwave-induced tissue heating (127). Accordingly, the water content and permittivity of these tissues (which, for example, is approximately half for normal lung and bone tissue what it is for kidney) may necessitate equipment optimization (128). Similarly, for ultrasound, mechanical properties (eg, density, bulk, and shear moduli) have been shown to influence temperature increases. Differences in refractive index may play a role in the penetration of light for different tissues when using laser ablation. As such, continued investigation into the effect of tissue characteristics on heating will likely continue for all of these energy platforms to achieve device optimization.

Role of Computer Modeling in Understanding Tissue Heating Patterns

Computer models have been developed to simulate percutaneous treatment of focal tumors by predicting tissue heating patterns for various clinical situations (120,129,130). Existing experimental approaches to modeling single variables or scenarios have been limited in completely predicting thermal ablation given the heterogeneous target clinical population, the complex number of variable tissue parameters, the time-consuming approach of single variable interrogation, and the heterogeneity of tumor and background organ biology and physiology. Therefore, more recent investigation (120,130) has evolved to incorporate both single- and two-compartment finite element computer modeling as a more realistic and clinically relevant simulation for improving the understanding of tissue heating patterns and tissue-energy interactions. Advantages of computer modeling include the ability to interrogate individual parameters in isolation or in combination to clarify their potential influence on energy deposition and tissue heating over a wide and clinically relevant physiologic range, the ability to separate out the specific environments in which certain variables demonstrate a more dominant effect, and the ability to characterize the effects of differences in tissue and tumor characteristics, especially at the tumor margin. This strategy may be helpful in better understanding heating for specific tumor and organ situations and, therefore, may improve RF predictability. Nevertheless, although preliminary results with computer modeling have been useful, predictive accuracy and clinical validation of these results are needed. Successful validation with subsequent translation to clinically relevant large-animal models will establish greater predictability of thermal coagulation and set the stage for rapid clinical translation and subsequent implementation.

Combining Percutaneous Ablation with Other Therapies

Expand

While substantial efforts have been made in modifying ablation systems and the biologic environment to improve the clinical utility of percutaneous ablation, limitations in clinical efficacy persist. For example, with further long-term follow-up of patients undergoing ablation therapy, there has been an increased incidence of detection of progressive local tumor growth for all tumor types and sizes despite initial indications of adequate therapy, suggesting that there are residual foci of viable untreated disease in a substantial number of cases (1,131). The ability to achieve complete and uniform eradication of all malignant cells remains a key barrier to clinical success, and therefore, strategies that can increase the completeness of tumor destruction with RF ablation, even for small lesions, are needed.

Investigators have sought to improve results by combining thermal ablation with adjuvant therapies, such as radiation and chemotherapy (5,10). Currently, thermal ablation only takes advantage of temperatures that are sufficient to induce coagulation necrosis by themselves (>50°C). However, owing to the exponential decrease in RF tissue heating, there is a steep thermal gradient in tissues surrounding an RF electrode. Hence, there is substantial flattening of the curve below 50°C, with a much larger tissue volume encompassed by the 45°C isotherm. Modeling studies demonstrate that if the threshold for cell death was decreased by as few as 5°C, tumor coagulation could be increased up to 1.5 cm (up to a 59% increase in spherical volume of the ablation zone) (132). Therefore, target tumors can be conceptually divided into three zones: *(a)* a central area, predominantly treated by thermal ablation, that undergoes heat-induced coagulation necrosis; *(b)* a peripheral rim that undergoes reversible changes from sublethal hyperthermia; and *(c)* surrounding tumor or normal tissue that is unaffected by focal ablation, though still exposed to adjuvant systemic therapies.

Several studies have demonstrated that tumor death can be enhanced by combining RF thermal therapy with adjuvant chemotherapy or radiosensitizers. The goal of this combined approach is to increase tumor destruction occurring within the sizable peripheral zone of sublethal temperatures (ie, largely reversible cell damage induced by mildly elevating tissue temperatures to 41°–45°C) surrounding the heat-induced coagulation (133) (Fig 12). Additional advantages of combined therapy may also include creating a more complete area of tumor destruction by filling in untreated gaps within the ablation zone and reducing the duration or course of therapy (a process that currently takes hours to treat larger tumors, with many protocols requiring repeat sessions).

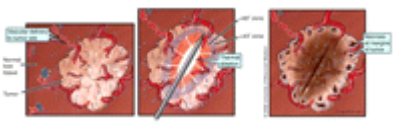

View larger version:

In this page In a new window

Download as PowerPoint Slide

Figure 12:

Illustrations show method for combining thermal ablation with targeted drug delivery. Left: Drugs are brought to the tumor site as part of normal circulation. Middle: Temperature elevations inside the ablation zone facilitate local

drug release, which then accumulates in the sublethal region at the periphery of the ablation zone. Right: Net result is a larger zone of ablation than would be possible with ablation alone. (Printed with permission from the University of Wisconsin–Madison.)

Expand

Thermal ablation with chemotherapy.—Combining thermal ablation (predominantly with RF-based systems) with chemotherapy (free or contained within liposomes; administered through direct injection, intravenously, or intravascularly or intraarterially) increases the overall volume of tumor necrosis and intratumoral drug accumulation (133) (Fig 13). These effects occur preferentially in the peripheral zone of hyperemia surrounding the central zone of ablation and have been confirmed in large-animal tumor models, different tumor and tissue types, for different chemotherapeutic agents, and in a pilot clinical study, in primary and secondary hepatic malignancies (10,133) (Fig 14). In clinical cases, the treatment effect extended in most cases to encompass peritumoral liver and enabled the destruction of the difficult to treat 0.5–1.0-cm ablative margin (10).

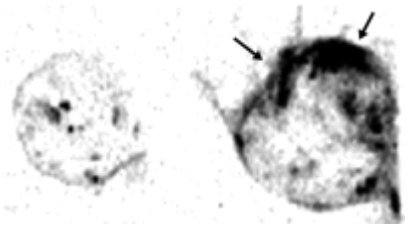

View larger version:
In this page In a new window
Download as PowerPoint Slide

Figure 13a:

Images show results of combination RF ablation and intravenous liposomal doxorubicin. **(a)** Autoradiographs of two paired tumors from the same animal 24 hours after intravenous administration of tritiated liposomes. Left: Without RF ablation. Right: With RF ablation immediately preceding liposome injection, the central zone with little uptake corresponds to the zone of RF coagulation, with a peripheral rim of increased liposome uptake (arrows). (Reprinted, with permission, from reference 95.) **(b)** Gross specimens of subcutaneous canine venereal sarcoma tumors. Right: RF ablation (12-minute application, 1-cm internally cooled electrode) combined with intravenous liposomal doxorubicin *(RF + Doxil)*. Left: RF ablation *(RF alone)*. In the tumor that underwent combined therapy, the central white zone (arrows) that corresponds to RF-induced coagulation is slightly (3-mm) larger and the peripheral red zone (arrowheads), which is frank coagulative necrosis, is dramatically increased in size (1.6 cm vs 0.7 cm). (Reprinted, with permission, from reference 134.)

Figure 13b:

Images show results of combination RF ablation and intravenous liposomal doxorubicin. **(a)** Autoradiographs of two paired tumors

Expand

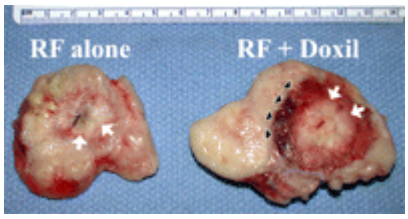

View larger version:
In this page In a new window
Download as PowerPoint Slide

from the same animal 24 hours after intravenous administration of tritiated liposomes. Left: Without RF ablation. Right: With RF ablation immediately preceding liposome injection, the central zone with little uptake corresponds to the zone of RF coagulation, with a peripheral rim of increased liposome uptake (arrows). (Reprinted, with permission, from reference 95.) **(b)** Gross specimens of subcutaneous canine venereal sarcoma tumors. Right: RF ablation (12-minute application, 1-cm internally cooled electrode) combined with intravenous liposomal doxorubicin *(RF + Doxil)*. Left: RF ablation *(RF alone)*. In the tumor that underwent combined therapy, the central white zone (arrows) that corresponds to RF-induced coagulation is slightly (3-mm) larger and the peripheral red zone (arrowheads), which is frank coagulative necrosis, is dramatically increased in size (1.6 cm vs 0.7 cm). (Reprinted, with permission, from reference 134.)

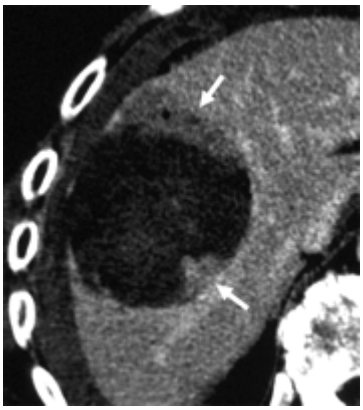

View larger version:
In this page In a new window
Download as PowerPoint Slide

Figure 14a:

CT images show increased tumor destruction with combined RF ablation and liposomal doxorubicin in an 82-year-old man with an 8.2-cm vascular hepatoma. **(a)** Image obtained immediately after RF ablation shows persistent regions of residual untreated tumor (arrows). **(b)** Image at 2-week follow-up shows interval increase in coagulation as the 1.5-cm inferior region of residual tumor and the 1.2-cm anteromedial portion of the tumor no longer enhance (arrowheads). A persistent nodule of viable tumor is shown (arrow), which was successfully treated with another course of RF ablation. **(c)** Image obtained immediately after RF ablation shows the persistence of a large vessel (arrows) in the nonenhancing ablated lesion. **(d)** Image at 2-week follow-up shows no enhancement in this region, and no vessel was seen on any of the three phases of contrast enhancement. No evidence of local tumor recurrence was identified at 48-month follow-up. (Reprinted, with permission, from reference 10.)

Expand

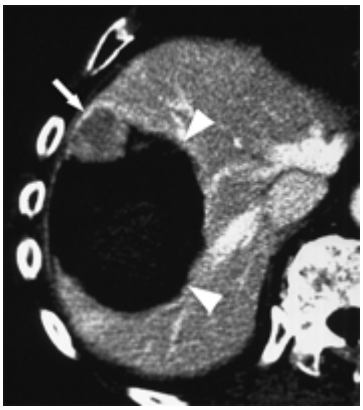

View larger version:

In this page In a new window

Download as PowerPoint Slide

Figure 14b:

CT images show increased tumor destruction with combined RF ablation and liposomal doxorubicin in an 82-year-old man with an 8.2-cm vascular hepatoma. **(a)** Image obtained immediately after RF ablation shows persistent regions of residual untreated tumor (arrows). **(b)** Image at 2-week follow-up shows interval increase in coagulation as the 1.5-cm inferior region of residual tumor and the 1.2-cm anteromedial portion of the tumor no longer enhance (arrowheads). A persistent nodule of viable tumor is shown (arrow), which was successfully treated with another course of RF ablation. **(c)** Image obtained immediately after RF ablation shows the persistence of a large vessel (arrows) in the nonenhancing ablated lesion. **(d)** Image at 2-week follow-up shows no enhancement in this region, and no vessel was seen on any of the three phases of contrast enhancement. No evidence of local tumor recurrence was identified at 48-month follow-up. (Reprinted, with permission, from reference 10.)

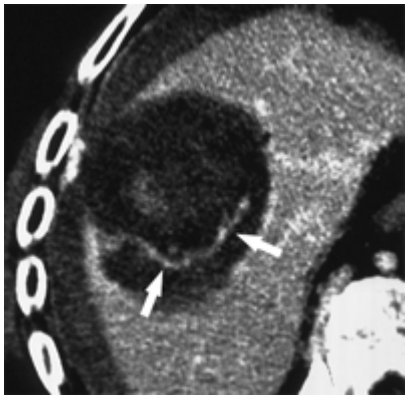

View larger version:

In this page In a new window

Download as PowerPoint Slide

Figure 14c:

CT images show increased tumor destruction with combined RF ablation and liposomal doxorubicin in an 82-year-old man with an 8.2-cm vascular hepatoma. **(a)** Image obtained immediately after RF ablation shows persistent regions of residual untreated tumor (arrows). **(b)** Image at 2-week follow-up shows interval increase in coagulation as the 1.5-cm inferior region of residual tumor and the 1.2-cm anteromedial portion of the tumor no longer enhance (arrowheads). A persistent nodule of viable tumor is shown (arrow), which was successfully treated with another course of RF ablation. **(c)** Image obtained immediately after RF ablation shows the persistence of a large vessel (arrows) in the nonenhancing ablated lesion. **(d)** Image at 2-week follow-up shows no enhancement in this region, and no vessel was seen on any of the three phases of contrast enhancement. No evidence of local tumor

recurrence was identified at 48-month follow-up. (Reprinted, with permission, from reference 10.)

Expand

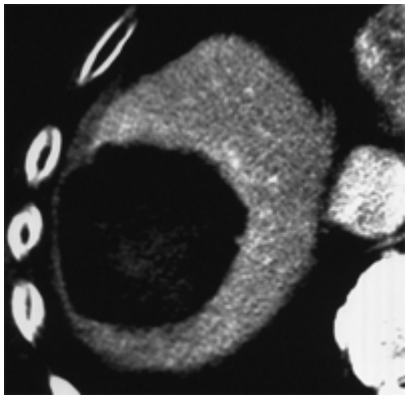

View larger version:
In this page In a new window
Download as PowerPoint Slide

Figure 14d:
CT images show increased tumor destruction with combined RF ablation and liposomal doxorubicin in an 82-year-old man with an 8.2-cm vascular hepatoma. **(a)** Image obtained immediately after RF ablation shows persistent regions of residual untreated tumor (arrows). **(b)** Image at 2-week follow-up shows interval increase in coagulation as the 1.5-cm inferior region of residual tumor and the 1.2-cm anteromedial portion of the tumor no longer enhance (arrowheads). A persistent nodule of viable tumor is shown (arrow), which was successfully treated with another course of RF ablation. **(c)** Image obtained immediately after RF ablation shows the persistence of a large vessel (arrows) in the nonenhancing ablated lesion. **(d)** Image at 2-week follow-up shows no enhancement in this region, and no vessel was seen on any of the three phases of contrast enhancement. No evidence of local tumor recurrence was identified at 48-month follow-up. (Reprinted, with permission, from reference 10.)

The underlying mechanisms of this synergy are multifactorial. Improved intratumoral drug delivery occurs with use of a liposomal carrier owing to increased circulation time, increased drug release with thermosensitive liposome types, and the well-documented vascular effects of sublethal hyperthermia (eg, vascular dilatation and increased endothelial permeability) in the peripheral treatment zone (135). Additionally, the cytotoxic effects of the chemotherapy agent combine with the heat-induced reduction in cellular reparative mechanisms to increase apoptosis (54). Finally, study results suggest that there are independent heat-related cytotoxic effects of the liposome itself (54). This preliminary success with combination therapy may be augmented by the development of new targeting vehicles, including several polymer-based temperature-dependent delivery systems currently under investigation (136).

Thermal ablation with radiation therapy.—Investigators have begun exploring combining RF ablation and radiation therapy with promising results. Previous data in the literature have demonstrated increased tumor destruction with external beam radiation therapy and low-temperature hyperthermia (137). Findings in experimental animal studies have demonstrated increased tumor necrosis, reduced tumor growth, and improved animal survival with

combined therapy when compared with either therapy alone (138,139) (Fig 15). Preliminary clinical studies in primary lung malignancies confirm the synergistic effects of these therapies (5). Potential causes for the synergy include the sensitization of the tumor to subsequent radiation owing to the increased oxygenation resulting from hyperthermia-induced increased blood flow to the tumor (140). Another possible mechanism, which has been seen in animal tumor models, is a radiation-induced inhibition of repair and recovery and increased free radical formation (54). Recent work with immunohistochemical staining after combination therapy with RF ablation and external beam radiation has demonstrated an increase in markers of oxidative and nitrosative stress (137). Future research is needed to identify the optimal temperature for ablation, the optimal radiation dose, and the most effective method of administering radiation therapy (eg, external beam radiation therapy, brachytherapy, or yttrium microspheres) on an organ-by-organ basis.

Figure 15a:

Combining RF ablation with external beam radiation for treatment of subcutaneously implanted R3230 rat breast tumors (arrowheads). **(a)** Left: Before treatment. Middle: Immediately after RF ablation combined with external beam radiation. Right: At 120-day follow-up. Posttreatment images show complete tumor dissolution. **(b)** Kaplan-Meier analysis shows increased animal survival with combination therapy *(RF + XRT)* compared with RF ablation alone *(RF)*, external beam radiation along *(XRT)*, and no treatment *(Control)*. *Tx* = treatment. (Reprinted, with permission, from reference 139.)

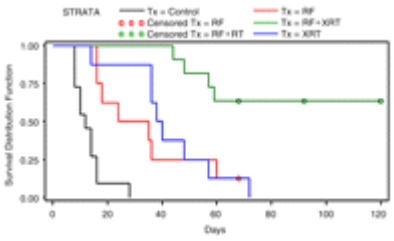

Figure 15b:

Combining RF ablation with external beam radiation for treatment of subcutaneously implanted R3230 rat breast tumors (arrowheads). **(a)** Left: Before treatment. Middle: Immediately after RF ablation combined with external beam radiation. Right: At 120-day follow-up. Posttreatment images show complete tumor dissolution. **(b)** Kaplan-Meier analysis shows increased animal survival with combination therapy *(RF + XRT)* compared with RF ablation alone *(RF)*, external beam radiation along *(XRT)*, and no treatment *(Control)*. *Tx* = treatment. (Reprinted, with permission, from reference 139.)

Expand

Conclusion

Minimally invasive percutaneous ablation has been well recognized as an important tool in the treatment of focal malignancies. Numerous studies over the last 2 decades have characterized many of the basic principles underlying ablative therapies. This article provides an overview of the basic principles of percutaneous tumor ablation and describes the equipment and technologic modifications that have been developed to further improve clinical success of this therapy. Researchers are now looking to optimize these devices for improved energy delivery to specific organ systems or tumor types, to enhance modeling capabilities to reduce development time and improve predictive abilities, and to develop combination therapies to further improve the clinical effectiveness of minimally invasive thermal ablation therapies.

Essentials

• Minimally invasive tumor ablation uses thermal- or chemical-based technologies to induce cellular death within the focal target tumor, ideally including an additional 0.5–1.0-cm ablative margin of normal-appearing parenchyma, while limiting damage to large amounts of normal tissue.

• Thermal ablation therapies, such as radiofrequency, microwave, and laser, use the energy-tissue interaction generated around an inserted applicator to adequately heat the target cells to induce irreversible injury (50°–54°C for 4–6 minutes is a commonly used endpoint).

• It is critical for radiologists to be familiar with advances in ablative technology, including the development of varying designs in electrodes and other applicators, generators, and energy application algorithms.

• Ablative technologies that are in development have the potential to improve upon current therapies by improving treatment of perivascular tumor tissue and reducing heat-related injuries (ie, irreversible electroporation) or making ablative procedures even less invasive (ie, high-intensity focused ultrasound).

• Combining tumor ablation with adjuvant therapies, such as chemo- or radiation therapy, has the potential to increase the size of the ablation zone and improve overall completeness of treatment.

Footnotes

Received September 12, 2008; revision requested November 12; revision received January 12, 2010; accepted January 20; final version accepted March 13; final review by M.A. August 27.

C.L.B. is a shareholder in and consultant for Neuwave Medical. F.T.L. is a shareholder in Neuwave Medical. S.N.G. receives research support from AngioDynamics.

Abbreviations:

IRE = irreversible electroporation
RF = radiofrequency

References

1.Solbiati L , Ierace T , Cova L , Zaid S , Imparato S . Ten-year experience in nonsurgical treatment of “intermediate” hepatocellular carcinoma in cirrhotic patients: long-term survival and causes of death [abstr]. In: *Radiological Society of North America scientific assembly and annual meeting program*. Oak Brook, Ill: Radiological Society of North America, 2006;359. **Search Google Scholar**

2.Livraghi T , Solbiati L , Meloni MF , Gazelle GS , Halpern EF , Goldberg SN . Treatment of focal liver tumors with percutaneous radio-frequency ablation: complications encountered in a multicenter study. *Radiology* 2003;**226**(2):441–451. **Abstract/FREE Full Text**

3.Gillams AR , Lees WR . Five-year survival following radiofrequency ablation of small, solitary, hepatic colorectal metastases. *J Vasc Interv Radiol* 2008;**19**(5):712–717. **CrossRef** **Medline**

4.Gervais DA , McGovern FJ , Arellano RS , McDougal WS , Mueller PR . Renal cell carcinoma: clinical experience and technical success with radio-frequency ablation of 42 tumors. *Radiology* 2003;**226**(2):417–424. **Abstract/FREE Full Text**

5.Dupuy DE , DiPetrillo T , Gandhi S , et al. Radiofrequency ablation followed by conventional radiotherapy for medically inoperable stage I non-small cell lung cancer. *Chest* 2006;**129**(3):738–745. **Abstract/FREE Full Text**

6.Callstrom MR , Atwell TD , Charboneau JW , et al. Painful metastases involving bone: percutaneous image-guided cryoablation—prospective trial interim analysis. *Radiology* 2006;**241**(2):572–580. **Abstract/FREE Full Text**

7.Yamakado K , Nakatsuka A , Takaki H , et al. Early-stage hepatocellular carcinoma: radiofrequency ablation combined with chemoembolization versus hepatectomy. *Radiology* 2008;**247**(1):260–266. **Abstract/FREE Full Text**

8.Takaki H , Yamakado K , Nakatsuka A , et al. Radiofrequency ablation combined with chemoembolization for the treatment of hepatocellular carcinomas 5 cm or smaller: risk factors for local tumor progression. *J Vasc Interv Radiol* 2007;**18**(7):856–861. **CrossRef** **Medline**

9.Jain SK , Dupuy DE , Cardarelli GA , Zheng Z , DiPetrillo TA . Percutaneous radiofrequency ablation of pulmonary malignancies: combined treatment with brachytherapy. *AJR Am J Roentgenol* 2003;**181**(3):711–715. **Abstract/FREE Full Text**

10.Goldberg SN , Kamel IR , Kruskal JB , et al. Radiofrequency ablation of hepatic tumors: increased tumor destruction with adjuvant liposomal doxorubicin therapy. *AJR Am J Roentgenol* 2002;**179**(1):93–101. **Abstract/FREE Full Text**

11.Shimada K , Sakamoto Y , Esaki M , Kosuge T . Role of the width of the surgical margin in a hepatectomy for small hepatocellular carcinomas eligible for percutaneous local ablative therapy. *Am J Surg* 2008;**195**(6):775–781. **CrossRef** **Medline**

12.Dodd GD 3rd., Soulen MC , Kane RA , et al. Minimally invasive treatment of malignant hepatic tumors: at the threshold of a major breakthrough. *RadioGraphics* 2000;**20**(1):9–27. **Abstract/FREE Full Text**

13.Lencioni R , Cioni D , Crocetti L , et al. Early-stage hepatocellular carcinoma in patients with cirrhosis: long-term results of percutaneous image-guided radiofrequency ablation. *Radiology* 2005;**234**(3):961–967. **Abstract/FREE Full Text**

14.Gervais DA , McGovern FJ , Arellano RS , McDougal WS , Mueller PR . Radiofrequency ablation of renal cell carcinoma. I. Indications, results, and role in patient management over a 6-year period and ablation of 100 tumors. *AJR Am J Roentgenol* 2005;**185**(1):64–71. **Abstract/FREE Full Text**

15.Lencioni R , Crocetti L , Cioni R , et al. Response to radiofrequency ablation of pulmonary tumours: a prospective, intention-to-treat, multicentre clinical trial (the RAPTURE study). *Lancet Oncol* 2008;**9**(7):621–628. **CrossRef** **Medline**

16.Hiraki T , Gobara H , Iishi T , et al. Percutaneous radiofrequency ablation for clinical stage I non-small cell lung cancer: results in 20 nonsurgical candidates. *J Thorac Cardiovasc Surg* 2007;**134**(5):1306–1312. **Abstract/FREE Full Text**

17.Callstrom MR , Charboneau JW . Image-guided palliation of painful metastases using percutaneous ablation. *Tech Vasc Interv Radiol* 2007;**10**(2):120–131. **CrossRef** **Medline**

18.Gillams A , Cassoni A , Conway G , Lees W . Radiofrequency ablation of neuroendocrine liver metastases: the Middlesex experience. *Abdom Imaging* 2005;**30**(4):435–441. **CrossRef** **Medline**

19.Dodd GD 3rd., Frank MS , Aribandi M , Chopra S , Chintapalli KN . Radiofrequency thermal ablation: computer analysis of the size of the thermal injury created by overlapping ablations. *AJR Am J Roentgenol* 2001;**177**(4):777–782. **Abstract/FREE Full Text**

20.Blendis L . Percutaneous ethanol ablation of small hepatocellular carcinomas: twenty years on. *Gastroenterology* 2006;**130**(1):280–282; discussion 282. **CrossRef** **Medline**

21.Taniguchi M , Kim SR , Imoto S , et al. Long-term outcome of percutaneous ethanol injection therapy for minimum-sized hepatocellular carcinoma. *World J Gastroenterol* 2008;**14**(13):1997–2002. **CrossRef** **Medline**

22.Mazzanti R , Arena U , Pantaleo P , et al. Survival and prognostic factors in patients with hepatocellular carcinoma treated by percutaneous ethanol injection: a 10-year experience. *Can J Gastroenterol* 2004;**18**(10):611–618. **Medline**

23.Andriulli A , de Sio I , Solmi L , et al. Survival of cirrhotic patients with early hepatocellular carcinoma treated by percutaneous ethanol injection or liver transplantation. *Liver Transpl* 2004;**10**(11):1355–1363. **CrossRef** **Medline**

24.Lin SM , Lin CJ , Lin CC , Hsu CW , Chen YC . Randomised controlled trial comparing percutaneous radiofrequency thermal ablation, percutaneous ethanol injection, and percutaneous acetic acid injection to treat hepatocellular carcinoma of 3 cm or less. *Gut* 2005;**54**(8):1151–1156. **Abstract/FREE Full Text**

25.Tsai WL , Cheng JS , Lai KH , et al. Clinical trial: percutaneous acetic acid injection vs. percutaneous ethanol injection for small hepatocellular carcinoma—a long-term follow-up study. *Aliment Pharmacol Ther* 2008;**28**(3):304–311. **CrossRef** **Medline**

26.Fukumoto K , Kojima T , Tomonari H , Kontani K , Murai S , Tsujimoto F . Ethanol injection sclerotherapy for Baker's cyst, thyroglossal duct cyst, and branchial cleft cyst. *Ann Plast Surg* 1994;**33**(6):615–619. **CrossRef** **Medline**

27.Hsieh CL , Shiau CS , Lo LM , Hsieh TT , Chang MY . Effectiveness of ultrasound-guided aspiration and sclerotherapy with 95% ethanol for treatment of recurrent ovarian endometriomas. *Fertil Steril* 2009;**91**(6):2709–2713. **CrossRef** **Medline**

28.Monchik JM , Donatini G , Iannuccilli J , Dupuy DE . Radiofrequency ablation and percutaneous ethanol injection treatment for recurrent local and distant well-differentiated thyroid carcinoma. *Ann Surg* 2006;**244**(2):296–304. **CrossRef** **Medline**

29.Livraghi T , Giorgio A , Marin G , et al. Hepatocellular carcinoma and cirrhosis in 746 patients: long-term results of percutaneous ethanol injection. *Radiology* 1995;**197** (1):101–108. **Abstract/FREE Full Text**

30.Shiina S , Tagawa K , Niwa Y , et al. Percutaneous ethanol injection therapy for hepatocellular carcinoma: results in 146 patients. *AJR Am J Roentgenol* 1993;**160** (5):1023–1028. **Abstract/FREE Full Text**

31.Shiina S , Tagawa K , Unuma T , et al. Percutaneous ethanol injection therapy for hepatocellular carcinoma: a histopathologic study. *Cancer* 1991;**68**(7):1524–1530. **Search Google Scholar**

32.Kawano M . An experimental study of percutaneous absolute ethanol injection therapy for small hepatocellular carcinoma: effects of absolute ethanol on the healthy canine liver. *Gastroenterol Jpn* 1989;**24**(6):663–669. **Medline**

33.Giovannini M , Seitz JF . Ultrasound-guided percutaneous alcohol injection of small liver metastases: results in 40 patients. *Cancer* 1994;**73**(2):294–297. **CrossRef** **Medline**

34.Ohnishi K , Ohyama N , Ito S , Fujiwara K . Small hepatocellular carcinoma: treatment with US-guided intratumoral injection of acetic acid. *Radiology* 1994;**193**(3):747–752. **Abstract/FREE Full Text**

35.Ohnishi K . Comparison of percutaneous acetic acid injection and percutaneous ethanol injection for small hepatocellular carcinoma. *Hepatogastroenterology* 1998;**45**(suppl 3):1254–1258. **Medline**

36.Nilsson E , von Euler H , Berendson J , et al. Electrochemical treatment of tumours. *Bioelectrochemistry* 2000;**51**(1):1–11. **CrossRef** **Medline**

37.Shafirstein G , Hennings L , Kaufmann Y , et al. Conductive interstitial thermal therapy (CITT) device evaluation in VX2 rabbit model. *Technol Cancer Res Treat* 2007;**6** (3):235–246. **Medline**

38.Dobbins C , Wemyss-Holden SA , Cockburn J , Maddern GJ . Bimodal electric tissue ablation-modified radiofrequency ablation with a Le Veen electrode in a pig model. *J Surg Res* 2008;**144**(1):111–116. **CrossRef** **Medline**

39.Goldberg SN , Gazelle GS , Mueller PR . Thermal ablation therapy for focal malignancy: a unified approach to underlying principles, techniques, and diagnostic imaging guidance. *AJR Am J Roentgenol* 2000;**174**(2):323–331. **FREE Full Text**

40.Georgiades CS , Hong K , Bizzell C , Geschwind JF , Rodriguez R . Safety and efficacy of CT-guided percutaneous cryoablation for renal cell carcinoma. *J Vasc Interv Radiol* 2008;**19**(9):1302–1310. **CrossRef** **Medline**

41.Rewcastle JC , Sandison GA , Saliken JC , Donnelly BJ , McKinnon JG . Considerations during clinical operation of two commercially available cryomachines. *J Surg Oncol* 1999;**71**(2):106–111. **CrossRef** **Medline**

42.Rewcastle JC , Sandison GA , Muldrew K , Saliken JC , Donnelly BJ . A model for the time dependent three-dimensional thermal distribution within iceballs surrounding multiple cryoprobes. *Med Phys* 2001;**28**(6):1125–1137. **Medline**

43.Permpongkosol S , Nicol TL , Link RE , et al. Differences in ablation size in porcine kidney, liver, and lung after cryoablation using the same ablation protocol. *AJR Am J Roentgenol* 2007;**188**(4):1028–1032. **Abstract/FREE Full Text**

44.Hinshaw JL , Sampson L , Lee FT Jr., Laeseke PF , Brace CL . Does selective intubation increase ablation zone size during pulmonary cryoablation? *J Vasc Interv Radiol* 2008;**19**(10):1497–1501. **CrossRef** **Medline**

45.Wang H , Littrup PJ , Duan Y , Zhang Y , Feng H , Nie Z . Thoracic masses treated with percutaneous cryotherapy: initial experience with more than 200 procedures. *Radiology* 2005;**235**(1):289–298. **Abstract/FREE Full Text**

46.Kim C , O'Rourke AP , Mahvi DM , Webster JG . Finite-element analysis of ex vivo and in vivo hepatic cryoablation. *IEEE Trans Biomed Eng* 2007;**54**(7):1177–1185. **CrossRef** **Medline**

47.Littrup PJ . How I do it: cryoablation [abstr]. In: *Radiological Society of North America scientific assembly and annual meeting program*. Oak Brook, Ill: Radiological Society of North America, 2005;70. **Search Google Scholar**

48.Trembley B , Ryan T , Strohbehn J . Interstitial hyperthermia: physics, biology, and clinical aspects. In: *Hyperthermia and oncology*. **Vol 3**. Utrecht, the Netherlands: VSP, 1992;11–98. Search Google Scholar

49.Seegenschmiedt MH , Brady LW , Sauer R . Interstitial thermoradiotherapy: review on technical and clinical aspects. *Am J Clin Oncol* 1990;**13**(4):352–363. Medline

50.Larson TR , Bostwick DG , Corica A . Temperature-correlated histopathologic changes following microwave thermoablation of obstructive tissue in patients with benign prostatic hyperplasia. *Urology* 1996;**47**(4):463–469. CrossRef Medline

51.Goldberg SN , Gazelle GS , Compton CC , Mueller PR , Tanabe KK . Treatment of intrahepatic malignancy with radiofrequency ablation: radiologic-pathologic correlation. *Cancer* 2000;**88**(11):2452–2463. CrossRef Medline

52.Zervas NT , Kuwayama A . Pathological characteristics of experimental thermal lesions: comparison of induction heating and radiofrequency electrocoagulation. *J Neurosurg* 1972;**37**(4):418–422. Medline

53.Thomsen S . Pathologic analysis of photothermal and photomechanical effects of laser-tissue interactions. *Photochem Photobiol* 1991;**53**(6):825–835. Medline

54.Solazzo SA , Ahmed M , Schor-Bardach R , et al. Liposomal doxorubicin increases radiofrequency ablation-induced tumor destruction by increasing cellular oxidative and nitrative stress and accelerating apoptotic pathways. *Radiology* 2010;**255**(1):62–74. Abstract/FREE Full Text

55.Goldberg SN , Gazelle GS , Halpern EF , Rittman WJ , Mueller PR , Rosenthal DI . Radiofrequency tissue ablation: importance of local temperature along the electrode tip exposure in determining lesion shape and size. *Acad Radiol* 1996;**3**(3):212–218. CrossRef Medline

56.Mertyna P , Dewhirst MW , Halpern E , Goldberg W , Goldberg SN . Radiofrequency ablation: the effect of distance and baseline temperature on thermal dose required for coagulation. *Int J Hyperthermia* 2008;**24**(7):550–559. CrossRef Medline

57.Mertyna P , Hines-Peralta A , Liu ZJ , Halpern E , Goldberg W , Goldberg SN . Radiofrequency ablation: variability in heat sensitivity in tumors and tissues. *J Vasc Interv Radiol* 2007;**18**(5):647–654. CrossRef Medline

58.Haemmerich D , Pilcher TA . Convective cooling affects cardiac catheter cryoablation and radiofrequency ablation in opposite directions. *Conf Proc IEEE Eng Med Biol Soc* 2007;**2007**:1499–1502. Medline

59.Ring ME , Huang SK , Gorman G , Graham AR . Determinants of impedance rise during catheter ablation of bovine myocardium with radiofrequency energy. *Pacing Clin Electrophysiol* 1989;**12**(9):1502–1513. CrossRef Medline

60.Goldberg SN , Gazelle GS , Solbiati L , Rittman WJ , Mueller PR . Radiofrequency tissue ablation: increased lesion diameter with a perfusion electrode. *Acad Radiol* 1996;**3**(8):636–644. CrossRef Medline

61.Leveillee RJ , Hoey MF , Hulbert JC , Mulier P , Lee D , Jesserun J . Enhanced radiofrequency ablation of canine prostate utilizing a liquid conductor: the virtual electrode. *J Endourol* 1996;**10**(1):5–11. CrossRef Medline

62.Lorentzen T . The loop electrode: in vitro evaluation of a device for ultrasound-guided interstitial tissue ablation using radiofrequency electrosurgery. *Acad Radiol* 1996;**3**(3):219–224. CrossRef Medline

63.Lencioni R , Goletti O , Armillotta N , et al. Radio-frequency thermal ablation of liver metastases with a cooled-tip electrode needle: results of a pilot clinical trial. *Eur Radiol* 1998;**8**(7):1205–1211. CrossRef Medline

64.Haemmerich D , Chachati L , Wright AS , Mahvi DM , Lee FT Jr., Webster JG . Hepatic radiofrequency ablation with internally cooled probes: effect of coolant temperature on lesion size. *IEEE Trans Biomed Eng* 2003;**50**(4):493–500. CrossRef Medline

65.Goldberg SN , Solbiati L , Hahn PF , et al. Large-volume tissue ablation with radio frequency by using a clustered, internally cooled electrode technique: laboratory and clinical experience in liver metastases. *Radiology* 1998;**209**(2):371–379. Abstract/FREE Full Text

66.Gulesserian T , Mahnken AH , Schernthaner R , et al. Comparison of expandable electrodes in percutaneous radiofrequency ablation of renal cell carcinoma. *Eur J Radiol* 2006;**59**(2):133–139. CrossRef Medline

67.Pereira PL , Trübenbach J , Schenk M , et al. Radiofrequency ablation: in vivo comparison of four commercially available devices in pig livers. *Radiology* 2004;**232**(2):482–490. Abstract/FREE Full Text

68.Brieger J , Pereira PL , Trübenbach J , et al. In vivo efficiency of four commercial monopolar radiofrequency ablation systems: a comparative experimental study in pig liver. *Invest Radiol* 2003;**38**(10):609–616. Medline

69.Buscarini E , Buscarini L . Radiofrequency thermal ablation with expandable needle of focal liver malignancies: complication report. *Eur Radiol* 2004;**14**(1):31–37. CrossRef Medline

70.Shibata T , Shibata T , Maetani Y , Isoda H , Hiraoka M . Radiofrequency ablation for small hepatocellular carcinoma: prospective comparison of internally cooled electrode and expandable electrode. *Radiology* 2006;**238**(1):346–353. Abstract/FREE Full Text

71.Steinke K , King J , Glenn D , Morris DL . Percutaneous radiofrequency ablation of lung tumors: difficulty withdrawing the hooks resulting in a split needle. *Cardiovasc Intervent Radiol* 2003;**26**(6):583–585. Medline

72.McGahan JP , Gu WZ , Brock JM , Tesluk H , Jones CD . Hepatic ablation using bipolar radiofrequency electrocautery. *Acad Radiol* 1996;**3**(5):418–422. CrossRef Medline

73.Ritz JP , Lehmann KS , Reissfelder C , et al. Bipolar radiofrequency ablation of liver metastases during laparotomy: first clinical experiences with a new multipolar ablation concept. *Int J Colorectal Dis* 2006;**21**(1):25–32. CrossRef Medline

74.Burdío F , Güemes A , Burdío JM , et al. Hepatic lesion ablation with bipolar saline-enhanced radiofrequency in the audible spectrum. *Acad Radiol* 1999;**6**(11):680–686. CrossRef Medline

75.Frericks BB , Ritz JP , Roggan A , Wolf KJ , Albrecht T . Multipolar radiofrequency ablation of hepatic tumors: initial experience. *Radiology* 2005;**237**(3):1056–1062. Abstract/FREE Full Text

76.Gananadha S , Morris DL . Saline infusion markedly reduces impedance and improves efficacy of pulmonary radiofrequency ablation. *Cardiovasc Intervent Radiol* 2004;**27**(4):361–365. Medline

77.Solazzo SA , Liu Z , Lobo SM , et al. Radiofrequency ablation: importance of background tissue electrical conductivity—an agar phantom and computer modeling study. *Radiology* 2005;**236**(2):495–502. Abstract/FREE Full Text

78.Solazzo SA , Ahmed M , Liu Z , Hines-Peralta AU , Goldberg SN . High-power generator for radiofrequency ablation: larger electrodes and pulsing algorithms in bovine ex vivo and porcine in vivo settings. *Radiology* 2007;**242**(3):743–750. Abstract/FREE Full Text

79.Brace CL , Laeseke PF , Sampson LA , Frey TM , Mukherjee R , Lee FT Jr.Radiofrequency ablation with a high-power generator: device efficacy in an in vivo porcine liver model. *Int J Hyperthermia* 2007;**23**(4):387–394. CrossRef Medline

80.Goldberg SN , Stein MC , Gazelle GS , Sheiman RG , Kruskal JB , Clouse ME . Percutaneous radiofrequency tissue ablation: optimization of pulsed-radiofrequency technique to increase coagulation necrosis. *J Vasc Interv Radiol* 1999;**10**(7):907–916. Medline

81.Bardy GH , Sawyer PL , Johnson GW , Reichenbach DD . Radio-frequency ablation: effect of voltage and pulse duration on canine myocardium. *Am J Physiol* 1990;**258**(6 pt 2):H1899–H1905. Medline

82.Lee FT Jr., Haemmerich D , Wright AS , Mahvi DM , Sampson LA , Webster JG . Multiple probe radiofrequency ablation: pilot study in an animal model. *J Vasc Interv Radiol* 2003;**14**(11):1437–1442. Medline

83.Brace CL , Sampson LA , Hinshaw JL , Sandhu N , Lee FT Jr.Radiofrequency ablation: simultaneous application of multiple electrodes via switching creates larger, more

confluent ablations than sequential application in a large animal model. *J Vasc Interv Radiol* 2009;**20**(1):118–124. CrossRef Medline

84.Lee JM , Han JK , Kim HC , et al. Multiple-electrode radiofrequency ablation of in vivo porcine liver: comparative studies of consecutive monopolar, switching monopolar versus multipolar modes. *Invest Radiol* 2007;**42**(10):676–683. CrossRef Medline

85.Rhim H , Dodd GD 3rd., Chintapalli KN , et al. Radiofrequency thermal ablation of abdominal tumors: lessons learned from complications. *RadioGraphics* 2004;**24**(1):41–52. Abstract/FREE Full Text

86.Steinke K , Gananadha S , King J , Zhao J , Morris DL . Dispersive pad site burns with modern radiofrequency ablation equipment. *Surg Laparosc Endosc Percutan Tech* 2003;**13**(6):366–371. Medline

87.Schutt DJ , Haemmerich D . Sequential activation of a segmented ground pad reduces skin heating during radiofrequency tumor ablation: optimization via computational models. *IEEE Trans Biomed Eng* 2008;**55**(7):1881–1889. CrossRef Medline

88.Wolf FJ , Grand DJ , Machan JT , Dipetrillo TA , Mayo-Smith WW , Dupuy DE . Microwave ablation of lung malignancies: effectiveness, CT findings, and safety in 50 patients. *Radiology* 2008;**247**(3):871–879. Abstract/FREE Full Text

89.Wright AS , Sampson LA , Warner TF , Mahvi DM , Lee FT Jr.Radiofrequency versus microwave ablation in a hepatic porcine model. *Radiology* 2005;**236**(1):132–139. Abstract/FREE Full Text

90.Yang D , Converse MC , Mahvi DM , Webster JG . Measurement and analysis of tissue temperature during microwave liver ablation. *IEEE Trans Biomed Eng* 2007;**54**(1):150–155. CrossRef Medline

91.Brace CL , Laeseke PF , Sampson LA , Frey TM , van der Weide DW , Lee FT Jr.Microwave ablation with a single small-gauge triaxial antenna: in vivo porcine liver model. *Radiology* 2007;**242**(2):435–440. Abstract/FREE Full Text

Goldberg SN, Hahn PF, Tanabe KK, et al. Percutaneous radiofrequency tissue ablation: does perfusion-mediated tissue cooling limit coagulation necrosis? *J Vasc Interv Radiol* 1998;**9**(1 pt 1):101–111. Medline

93.Horkan C , Ahmed M , Liu Z , et al. Radiofrequency ablation: effect of pharmacologic modulation of hepatic and renal blood flow on coagulation diameter in a VX2 tumor model. *J Vasc Interv Radiol* 2004;**15**(3):269–274. Medline

Ahmed M, Lobo SM, Weinstein J, et al. Improved coagulation with saline solution pretreatment during radiofrequency tumor ablation in a canine model. *J Vasc Interv Radiol* 2002;**13**(7):717–724. Medline

95.Monsky WL , Kruskal JB , Lukyanov AN , et al. Radio-frequency ablation increases intratumoral liposomal doxorubicin accumulation in a rat breast tumor model. *Radiology* 2002;**224**(3):823–829. Abstract/FREE Full Text

96.Strickland AD , Clegg PJ , Cronin NJ , et al. Experimental study of large-volume microwave ablation in the liver. *Br J Surg* 2002;**89**(8):1003–1007. CrossRef Medline

97.Wang Y , Sun Y , Feng L , Gao Y , Ni X , Liang P . Internally cooled antenna for microwave ablation: results in ex vivo and in vivo porcine livers. *Eur J Radiol* 2008;**67**(2):357–361. CrossRef Medline

98.Brace CL . Microwave ablation technology: what every user should know. *Curr Probl Diagn Radiol* 2009;**38**(2):61–67. CrossRef Medline

99.Yu NC , Lu DS , Raman SS , et al. Hepatocellular carcinoma: microwave ablation with multiple straight and loop antenna clusters—pilot comparison with pathologic findings. *Radiology* 2006;**239**(1):269–275. Abstract/FREE Full Text

Ito K, Saito K, Yoshimura H, Aoyagi Y, Horita H. Coaxial-slot antenna for interstitial microwave thermal therapy and its application to clinical trial. *Conf Proc IEEE Eng Med Biol Soc* 2004;**4**:2526–2529. Medline

Shibata T, Iimuro Y, Yamamoto Y, et al. Small hepatocellular carcinoma: comparison of radio-frequency ablation and percutaneous microwave coagulation therapy. *Radiology* 2002;**223**(2):331–337. Abstract/FREE Full Text

Sun Y, Wang Y, Ni X, et al. Comparison of ablation zone between 915- and 2,450-MHz cooled-shaft microwave antenna: results in in vivo porcine livers. *AJR Am J Roentgenol* 2009;**192**(2):511–514. **Abstract/FREE Full Text**

Vogl TJ, Straub R, Eichler K, Woitaschek D, Mack MG. Malignant liver tumors treated with MR imaging–guided laser-induced thermotherapy: experience with complications in 899 patients (2,520 lesions). *Radiology* 2002;**225**(2):367–377. **Abstract/FREE Full Text**

104.Christophi C , Nikfarjam M , Malcontenti-Wilson C , Muralidharan V . Long-term survival of patients with unresectable colorectal liver metastases treated by percutaneous interstitial laser thermotherapy. *World J Surg* 2004;**28**(10):987–994. **CrossRef** **Medline**

105.Walser EM . Percutaneous laser ablation in the treatment of hepatocellular carcinoma with a tumor size of 4 cm or smaller: analysis of factors affecting the achievement of tumor necrosis. *J Vasc Interv Radiol* 2005;**16**(11):1427–1429. **Medline**

106.Stollberger R , Ascher PW , Huber D , Renhart W , Radner H , Ebner F . Temperature monitoring of interstitial thermal tissue coagulation using MR phase images. *J Magn Reson Imaging* 1998;**8**(1):188–196. **Medline**

107.Skinner MG , Iizuka MN , Kolios MC , Sherar MD . A theoretical comparison of energy sources—microwave, ultrasound and laser—for interstitial thermal therapy. *Phys Med Biol* 1998;**43**(12):3535–3547. **CrossRef** **Medline**

108.Heisterkamp J , van Hillegersberg R , Sinofsky E , IJzermans JN . Heat-resistant cylindrical diffuser for interstitial laser coagulation: comparison with the bare-tip fiber in a porcine liver model. *Lasers Surg Med* 1997;**20**(3):304–309. **CrossRef** **Medline**

109.Veenendaal LM , de Jager A , Stapper G , Borel Rinkes IH , van Hillegersberg R . Multiple fiber laser-induced thermotherapy for ablation of large intrahepatic tumors. *Photomed Laser Surg* 2006;**24**(1):3–9. **CrossRef** **Medline**

110.Kinsey AM , Tyreus PD , Rieke V , et al. Interstitial ultrasound applicators with dynamic angular control for thermal ablation of tumors under MR-guidance. *Conf Proc IEEE Eng Med Biol Soc* 2004;**4**:2496–2499. **Medline**

111.Deardorff DL , Diederich CJ . Axial control of thermal coagulation using a multi-element interstitial ultrasound applicator with internal cooling. *IEEE Trans Ultrason Ferroelectr Freq Control* 2000;**47**(1):170–178. **CrossRef** **Medline**

112.Barqawi AB , Crawford ED . Emerging role of HIFU as a noninvasive ablative method to treat localized prostate cancer. *Oncology (Williston Park)* 2008;**22**(2):123–129; discussion 129, 133, 137. **Medline**

113.Rubinsky B , Onik G , Mikus P . Irreversible electroporation: a new ablation modality—clinical implications. *Technol Cancer Res Treat* 2007;**6**(1):37–48. **Medline**

114.Lee EW , Loh CT , Kee ST . Imaging guided percutaneous irreversible electroporation: ultrasound and immunohistological correlation. *Technol Cancer Res Treat* 2007;**6**(4):287–294. **Medline**

115.Onik G , Mikus P , Rubinsky B . Irreversible electroporation: implications for prostate ablation. *Technol Cancer Res Treat* 2007;**6**(4):295–300. **Medline**

116.Rubinsky J , Onik G , Mikus P , Rubinsky B . Optimal parameters for the destruction of prostate cancer using irreversible electroporation. *J Urol* 2008;**180**(6):2668–2674. **CrossRef** **Medline**

117.Lu DS , Raman SS , Limanond P , et al. Influence of large peritumoral vessels on outcome of radiofrequency ablation of liver tumors. *J Vasc Interv Radiol* 2003;**14**(10):1267–1274. **Medline**

118.Hakimé A , Hines-Peralta A , Peddi H , et al. Combination of radiofrequency ablation with antiangiogenic therapy for tumor ablation efficacy: study in mice. *Radiology* 2007;**244**(2):464–470. **Abstract/FREE Full Text**

119.Livraghi T , Goldberg SN , Lazzaroni S , et al. Hepatocellular carcinoma: radiofrequency ablation of medium and large lesions. *Radiology* 2000;**214**(3):761–768. **Abstract/FREE Full Text**

120.Ahmed M , Liu Z , Humphries S , Goldberg SN . Computer modeling of the combined effects of perfusion, electrical conductivity, and thermal conductivity on tissue heating patterns in radiofrequency tumor ablation. *Int J Hyperthermia* 2008;**24** (7):577–588. CrossRef Medline

121.Goldberg SN , Ahmed M , Gazelle GS , et al. Radio-frequency thermal ablation with NaCl solution injection: effect of electrical conductivity on tissue heating and coagulation—phantom and porcine liver study. *Radiology* 2001;**219**(1):157–165. Abstract/FREE Full Text

122.Aubé C , Schmidt D , Brieger J , et al. Influence of NaCl concentrations on coagulation, temperature, and electrical conductivity using a perfusion radiofrequency ablation system: an ex vivo experimental study. *Cardiovasc Intervent Radiol* 2007;**30**(1):92–97. CrossRef Medline

123.Miao Y , Ni Y , Yu J , Marchal G . A comparative study on validation of a novel cooled-wet electrode for radiofrequency liver ablation. *Invest Radiol* 2000;**35**(7):438 –444. CrossRef Medline

124.Gillams AR , Lees WR . CT mapping of the distribution of saline during radiofrequency ablation with perfusion electrodes. *Cardiovasc Intervent Radiol* 2005;**28**(4):476–480. CrossRef Medline

125.Lee SJ , Choyke LT , Locklin JK , Wood BJ . Use of hydrodissection to prevent nerve and muscular damage during radiofrequency ablation of kidney tumors. *J Vasc Interv Radiol* 2006;**17**(12):1967–1969. CrossRef Medline

126.Laeseke PF , Sampson LA , Winter TC 3rd., Lee FT Jr.Use of dextrose 5% in water instead of saline to protect against inadvertent radiofrequency injuries. *AJR Am J Roentgenol* 2005;**184**(3):1026–1027. FREE Full Text

127.Schepps JL , Foster KR . The UHF and microwave dielectric properties of normal and tumour tissues: variation in dielectric properties with tissue water content. *Phys Med Biol* 1980;**25**(6):1149–1159. CrossRef Medline

128.Durick NA , Laeseke PF , Broderick LS , et al. Microwave ablation with triaxial antennas tuned for lung: results in an in vivo porcine model. *Radiology* 2008;**247** (1):80–87. Abstract/FREE Full Text

129.Haemmerich D , Tungjitkusolmun S , Staelin ST , Lee FT Jr., Mahvi DM , Webster JG . Finite-element analysis of hepatic multiple probe radio-frequency ablation. *IEEE Trans Biomed Eng* 2002;**49**(8):836–842. CrossRef Medline

130.dos Santos I , Haemmerich D , Pinheiro Cda S , da Rocha AF . Effect of variable heat transfer coefficient on tissue temperature next to a large vessel during radiofrequency tumor ablation. *Biomed Eng Online* 2008;**7**:21. CrossRef Medline

131.Rhim H , Dodd GD 3rd.Radiofrequency thermal ablation of liver tumors. *J Clin Ultrasound* 1999;**27**(5):221–229. CrossRef Medline

132.Liu Z , Lobo SM , Humphries S , et al. Radiofrequency tumor ablation: insight into improved efficacy using computer modeling. *AJR Am J Roentgenol* 2005;**184** (4):1347–1352. Abstract/FREE Full Text

133.Ahmed M , Goldberg SN . Combination radiofrequency thermal ablation and adjuvant IV liposomal doxorubicin increases tissue coagulation and intratumoural drug accumulation. *Int J Hyperthermia* 2004;**20**(7):781–802. CrossRef Medline

134.Ahmed M , Liu Z , Lukyanov AN , et al. Combination radiofrequency ablation with intratumoral liposomal doxorubicin: effect on drug accumulation and coagulation in multiple tissues and tumor types in animals. *Radiology* 2005;**235**(2):469–477. Abstract/FREE Full Text

135.Chen Q , Krol A , Wright A , Needham D , Dewhirst MW , Yuan F . Tumor microvascular permeability is a key determinant for antivascular effects of doxorubicin encapsulated in a temperature sensitive liposome. *Int J Hyperthermia* 2008;**24**(6):475–482. CrossRef Medline

136.Bae Y , Buresh RA , Williamson TP , Chen TH , Furgeson DY . Intelligent biosynthetic nanobiomaterials for hyperthermic combination chemotherapy and thermal drug targeting of HSP90 inhibitor geldanamycin. *J Control Release* 2007;**122**(1):16–23. CrossRef Medline

137.Algan O , Fosmire H , Hynynen K , et al. External beam radiotherapy and hyperthermia in the treatment of patients with locally advanced prostate carcinoma. *Cancer* 2000;**89**(2):399–403. Medline

138.Solazzo S , Mertyna P , Peddi H , Ahmed M , Horkan C , Goldberg SN . RF ablation with adjuvant therapy: comparison of external beam radiation and liposomal doxorubicin on ablation efficacy in an animal tumor model. *Int J Hyperthermia* 2008;**24**(7):560–567. CrossRef Medline

139.Horkan C , Dalal K , Coderre JA , et al. Reduced tumor growth with combined radiofrequency ablation and radiation therapy in a rat breast tumor model. *Radiology* 2005;**235**(1):81–88. Abstract/FREE Full Text

140.Mayer R , Hamilton-Farrell MR , van der Kleij AJ , et al. Hyperbaric oxygen and radiotherapy. *Strahlenther Onkol* 2005;**181**(2):113–123. CrossRef Medline

141.Brace CL . Microwave tissue ablation: biophysics, technology, and applications. *Crit Rev Biomed Eng* 2010;**38**(1):65–78. Medline

Articles citing this article

A Selective Review of Commonly Used Sonography-Guided Hyperthermic Ablative Technologies for Malignant Lesions of the Liver

Journal of Diagnostic Medical Sonography May 1, 2012 28:3 120-125

Abstract Full Text Full Text (PDF)

Hyperthermia in Bone Generated with MR Imaging-controlled Focused Ultrasound: Control Strategies and Drug Delivery

Radiology April 1, 2012 263:1 117-127

Abstract Full Text Full Text (PDF)

Science to Practice: What Do Molecular Biologic Studies in Rodent Models Add to Our Understanding of Interventional Oncologic Procedures including Percutaneous Ablation by Using Glyceraldehyde-3-Phosphate Dehydrogenase Antagonists?

Radiology March 1, 2012 262:3 737-739

Full Text Full Text (PDF)

Human Hepatocellular Carcinoma in a Mouse Model: Assessment of Tumor Response to Percutaneous Ablation by Using Glyceraldehyde-3-Phosphate Dehydrogenase Antagonists

Radiology March 1, 2012 262:3 834-845

Abstract Full Text Full Text (PDF)

Characterization of Irreversible Electroporation Ablation in In Vivo Porcine Liver

Am. J. Roentgenol. January 1, 2012 198:1 W62-W68

Abstract Full Text Full Text (PDF)

Science to Practice: Which Approaches to Combination Interventional Oncologic Therapy Hold the Greatest Promise of Obtaining Maximal Clinical Benefit?

Radiology December 1, 2011 261:3 667-669

Full Text Full Text (PDF)

Percutaneous Tumor Ablation for Hepatocellular Carcinoma

Am. J. Roentgenol. October 1, 2011 197:4 789-794

Abstract Full Text Full Text (PDF)